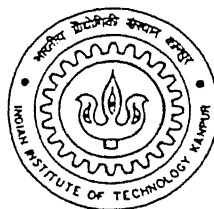


MULTIDIMENSIONAL TRANSIENT SIMULATION OF A FLAT PLATE SOLAR COLLECTOR

*A Thesis Submitted
in Partial Fulfillment of the Requirements
for the Degree of
Master of Technology*

by
Nikunj Kumar Srivastava



to the
Department of Mechanical Engineering
Indian Institute of Technology, Kanpur
April, 1998

22 SEP 1998 JME
CENTRAL LIBRARY
I. I. T. KANPUR

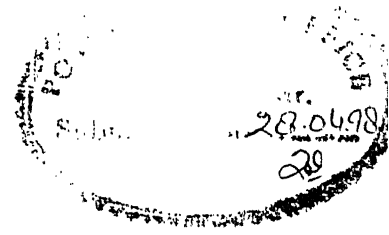
Acc. No. A 126255

Entered In System

ME-1998-M-SRI-MUL



A126255



Certificate

Certified that the work contained in the thesis entitled "*Multidimensional Transient Simulation of a Flat Plate Solar Collector*", by Mr. *Nikunj Kumar Srivastava*, has been carried out under my supervision and that this work has not been submitted elsewhere for a degree.

Keshav Kant
28.04.98

(Dr. Keshav Kant)

Professor,

Department of Mechanical Engineering,

Indian Institute of Technology,

Kanpur.

April, 1998

Abstract

This thesis presents a numerical model that has been developed for determination of thermal behavior of a solar collector. The model takes into account the multi-dimension and transient aspects that characterise the phenomena of heat transfer in a collector. The analysis of different elements of a flat plate solar collector, viz., cover, absorber plate, insulation and fluid has been coupled in a global algorithm. The algorithm is presented, herein, in the form of a flow chart. The analysis allows the prediction of instantaneous temperature distribution in various components of a collector while fluid is continuously flowing through it, as well as the performance and the influence of various parameters such as mass flow rates, inlet fluid temperature and plate tilt. However, the same analysis can be used to predict the influence of other parameters such as collector dimensions, material properties etc., also on the performance.

Acknowledgement

I take this opportunity to express my sense of gratitude to my supervisor Prof. Keshav Kant, to whom I owe more than I can possibly express, for his warm guidance that led me to the completion of this work. It was a great pleasure to work under him as a lot of care and affection was available through out. I shall ever remain grateful to him.

I express my deepest gratitude to my parents and other family members for their invaluable support and affection.

I would like to thank my friends Avi, Shivendra, Maneesh, Sandeep, Rajan, Sonal, Rahul, Sudhir, Atul Gupta, Mod Prakash, Santosh, and Deepak Tiwari for their warm affections and help to make my stay at IIT Kanpur a pleasant one. I Also thank Dobhal, Avi, Deepak, Thakre, Robert, Rahul, Sahai and Sonal for coming to my rescue during the final stages of the thesis.

Nikunj Kumar Srivastava

IIT Kanpur

April, 1998

Nomenclature

| | |
|-----------|---|
| A | area (m^2) |
| abs | absorbed |
| C | specific heat ($J.kg^{-1}.K^{-1}$) at constant pressure |
| D_i | inner diameter of duct (m) |
| D_o | outer diameter of duct (m) |
| h | heat tranfer coefficient ($W.m^{-2}.K^{-1}$) |
| i,j,k | indicator of i,j and k^{th} spatial position in x,y and z directions respectively |
| k | thermal conductivity ($W.m^{-1}.K^{-1}$) |
| I_o | solar radiation flux on the collector per unit area ($W.m^{-2}$) |
| \dot{m} | total fluid mass flow flux ($kg.s^{-1}$) |
| n | number of nodal points |
| N | number of ducts |
| q | rate of heat transfer per unit surface ($W.m^{-2}$) |
| Q | rate of heat transfer (W) |
| R | perimeter |
| S | amount of heat flux absorbed by the absorber plate ($W.m^{-2}$) |
| t | time (s) |
| x,y,z | spatial coordinates |

Greek Symbols

| | |
|------------|--|
| α | absorptivity of absorber plate |
| β | collector tilt (radian) |
| γ | surface azimuthal angle (radian) |
| δ | thickness (m) |
| ϵ | emissivity |
| ϕ | latitude (radian) |
| ρ | reflectivity, density (kg.m^{-3}) |
| θ | angle of incidence of radiation on a tilted surface |
| θ_2 | refraction angle (radian) |
| θ_z | angle of incidence of radiation on a horizontal surface |
| τ | transmissivity of glass cover |
| σ | Stefan-Boltzman constant ($= 5.67 \cdot 10^{-8} \text{ W.m}^{-2}.\text{K}^{-4}$) |
| η | efficiency |

Subscript

| | |
|----|-------------------|
| a | ambient |
| b | beam |
| c | cover |
| d | diffuse |
| f | fluid |
| i | insulation |
| g | air gap |
| in | inlet conditions |
| m | mean |
| o | output conditions |
| p | absorber plate |
| w | wind |

List of Figures

1. Figure 1.1 : Configuration of flat plate solar collector
2. Figure 3.1 : Discrete elements of different components
3. Figure 3.2 : Flow chart of simulation program
4. Figure 4.1 : Ambient temperature variation with the time of the day
5. Figure 4.2 : Incident solar flux on collector cover with the time of the day
6. Figure 4.3 : Comparison of the predicted rise in fluid temperature with experimental data
7. Figure 4.4 : Mean plate temperature along flow direction for different flow rates
8. Figure 4.5 : Rise in the fluid temperature with the time of the day for different flow rates
9. Figure 4.6 : Instantaneous efficiency with the time of the day for different flow rates
10. Figure 4.7 : Instantaneous energy distribution with the time of the day
11. Figure 4.8 : Instantaneous energy distribution with the time of the day
12. Figure 4.9 : Mean efficiency variation with the flow rate
13. Figure 4.10 : Rise in fluid temperature with time of the day for different tilt angles

14. Figure 4.11 : Rise in fluid temperature with time of the day for different tilt angles
15. Figure 4.12 : Mean efficiency variation with inlet fluid temperature

Contents

| | | |
|----------|---|-----------|
| 1 | Introduction | 1 |
| 1.1 | Importance of solar energy | 1 |
| 1.1.1 | Solar water heating | 2 |
| 1.1.2 | Solar cooking | 2 |
| 1.1.3 | Space heating | 2 |
| 1.1.4 | Conversion to electricity | 2 |
| 1.1.5 | Solar distillation | 3 |
| 1.2 | Solar collectors and their main components | 3 |
| 1.3 | Background Information | 4 |
| 1.4 | Scope of the Present Study | 5 |
| 2 | Problem Formulation | 8 |
| 2.1 | Solar Radiation | 8 |
| 2.2 | Governing Equations for the multidimensional and Transient Analysis | 9 |
| 2.2.1 | Cover | 10 |
| 2.2.2 | Plate | 11 |
| 2.2.3 | Insulation | 12 |
| 2.2.4 | Fluid | 12 |
| 2.3 | Efficiency of a Flat Plate Solar Collector | 13 |
| 3 | Numerical Modelling | 14 |
| 3.1 | Cover | 16 |
| 3.2 | Plate | 17 |
| 3.3 | Insulation | 19 |
| 3.4 | Fluid | 21 |

| | | |
|----------|---------------------------------------|-----------|
| 4 | Results and Discussion | 24 |
| 4.1 | Results | 24 |
| 4.2 | Conclusion | 36 |
| 4.3 | Suggestions for future work | 40 |
| A | Appendix | 41 |
| B | References | 43 |

Chapter 1

Introduction

1.1 Importance of solar energy

While conventional sources of energy can not be neglected, it is imperative to develop programmes in the area of renewable sources as they not only help conserve scarce conventional sources of energy, but also contribute immensely to the improvement of environment, employment generation, upgradation of health and hygiene, etc. The potential for energy generation from these sources -sun, wind , biomass, etc - is immense.

Taking a global energy view, it is felt that solar energy is one of the most promising alternate sources because of its diffuse nature and world wide availability. Solar energy has a great future in the tropical country like India, where many places receive a peak solar flux of the order of 1 kW/m^2 . The need for solar energy has become especially relevant in the wake of the energy crisis in the rural sector. In India, there are still 1,00,000 villages where darkness is not dispelled by electricity. These villages ,due to their remote location, are not likely to have access to electricity supply from the national grid for a very long time partly because of high initial cost of transmission. In the rural areas, domestic energy consumption, especially for cooking, constitute a significant part of energy demand. The other uses of energy are for lighting, water heating, irrigation, post harvesting operations and village industries like brick kilns, flour mills, rice mills and agro processing units. Some of

the viable uses of solar energies are as follows :

1.1.1 Solar water heating

Many flat plate and concentrating collectors have been designed for their usefulness in the water heating. They consists of a box with glass covers, covering a metallic absorber plate carrying water in the ducts. The water is heated by solar energy absorbed by the blackened absorber plate.

1.1.2 Solar cooking

A solar cooker can be easily designed and fabricated. The simplest type is a box with glass cover facing the sun. Mirrors can be provided to give some degree of concentration which would bring the food, to be cooked, up to cooking temperatures quickly.

1.1.3 Space heating

Space heating is generally employed in cold countries where keeping the house warm is a big problem. This is normally achieved by using solar air-heaters (active solar heating) or by designing the house itself to trap the solar energy(passive solar-heating).

1.1.4 Conversion to electricity

Electricity can be generated directly from sunlight with the help of solar photovoltaic (SPV) technology. The basis is the photoelectric effect. The atoms of certain materials such as selenium, possess electrons that are easily knocked out of place by light energy. Another metal that is in contact with the electron-emitting metal collects the electrons and passes them along into wires in a steady stream, while other electrons from the wires flow in to replace them. Thus, an electric current is established.

1.1.5 Solar distillation

One of the major problems in many parts of the world is the non-availability of fresh water. Solar stills can convert saline or brackish water into fresh potable water easily, by the process of evaporation and condensation.

Some other uses of solar energy worth mentioning are solar refrigeration and air conditioning, solar furnaces, solar pumps, heating sewage digestors in sewage treatment, solar pond, generation of mechanical power, drying grains or vegetables etc.

1.2 Solar collectors and their main components

In the last few decades, new solar collectors of different shapes have come up. The flat plate collectors have evoked considerable interest because they are the simplest among the solar energy collecting devices and have a wide range of potential for heating and cooling applications. They usually consists of the following components:

Absorber plate

It is a blackened metallic plate which is exposed to sun. It is made of a highly conducting material with a view to trap maximum amount of radiation incident upon it and transferring it to the fluid flowing through the tubes in contact with the absorber plate.

Cover plate

It is a glass plate usually placed over the absorber plate to reduce heat losses. It allows the short wavelength radiation from the sun to pass through it and impinge on the absorber plate. Due to the heating up of the absorber plate long wave radiations are produced. These radiations are prevented by the glass cover from passing into the atmosphere. Hence it leads to higher collection temperature for fixed heat losses. The cover plate may be one or two in number.

Fluid

It is a means to extract the heat absorbed by the absorber plate. This hot fluid may directly be used for heating purposes or may transfer its heat to another fluid through a heat exchanger.

Insulation

The bottom part of the absorber plate is separated from the ambient conditions by means of a layer of insulated material. This insulation prevents the loss of heat by the plate to the surroundings. Usually the insulation used are glass wool, wood wool, saw dust, thermocoal etc.

1.3 Background Information

In most of the current bibliography - Hottel and Woertz (1942), Duffie and Beckman (1980) - the thermal behaviour of solar collectors is calculated on the basis of models that do not take into account the multidimensional and transient nature of the phenomenon. When these aspects are analysed, the governing energy equations that characterize the thermal behavior of a solar collector are difficult to solve. Different models with simplified assumptions have appeared in an attempt to assess the transient behavior of a collector (Smith, 1986). These models, however, do not take into account the multidimensional and transient aspects of the problem.

Brian (1961) used a finite difference method of high order accuracy for the solution of three dimensional transient heat conduction problems. Thomas (1949) used an algorithm to solve elliptical problems in linear difference equations over a network. Consequently some work dealing with numerical simulation of solar collectors was carried out. Saito and Utaka (1984) presented numerical solutions for a solar water heater. They considered a transient one dimensional model. Chiou (1982) presented a two-dimensional steady model to study the nonuniformity in the fluid flow distribution. A multidimensional, but quasi steady analysis has been done by Agarwal (1996).

The conventional one-dimensional analysis for a flat plate solar collector with water as the heating fluid is based on the following assumptions :

1. Steady-state performance.
2. The headers cover a small area of the collector surface and therefore can be neglected.
3. The headers provide uniform flow to the tubes.
4. No absorption of solar energy by the glass covers in so far as it affects the losses from the collector.
5. One-dimensional heat flow through the covers.
6. Negligible temperature drop through the glass covers.
7. One dimensional heat flow through the bottom insulation.
8. The sky can be considered as a black body.
9. Temperature gradient around the tubes can be neglected.
10. Temperature gradient in the direction of flow and between the tubes can be treated independently.
11. Properties are independent of temperature.
12. Dust and dirt on the collector are negligible.
13. Shading of the collector plate is negligible.

1.4 Scope of the Present Study

The main objective of this study is to present a numerical simulation taking into account multidimensional and transient modelling of the different elements of a conventional flat plate solar collector , viz., cover, duct, plate etc and their coupling

in a global algorithm. The Finite difference technique has been employed for the solution of the governing partial differential equations.

The present work takes into account the multi-dimensional and transient aspects of a flat plate solar collector. Solar energy absorbed by the glass cover is also taken into account. This analysis, therefore, leads to the relaxation of five assumptions, viz., 1st, 4th, 5th, 7th and the 10th. Thus; it presents a more realistic physical model.

A computer program has been developed to predict the performance of a flat plate solar collector based on this model. The present work predicts the performance of a conventional flat plate solar collector for a given day, location, material properties and geometry. It also predicts the performance of the collector with variation in the following parameters :

- The time of the day
- Mass flow rate
- Plate tilt angle
- Fluid inlet temperature

While the effect of variation of one parameter, on the performance, is studied, other parameters are kept constant.

The configuration of flat plate solar collector (with dimensions) used in present analysis is shown in Figure 1.1. The collector has nine tubes and they are in line with the absorber plate.

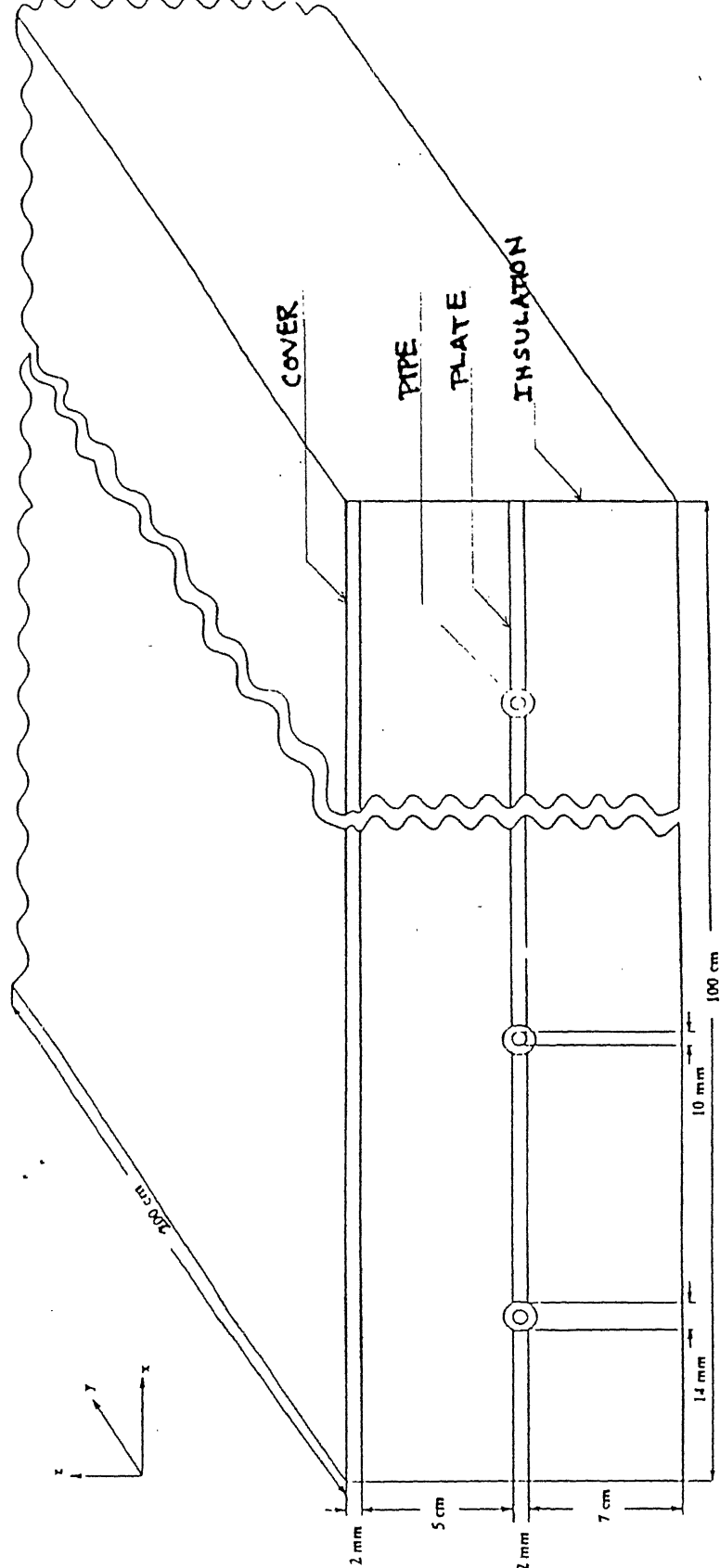


Figure 1.1 : Configuration of flat plate solar collector

Chapter 2

Problem Formulation

2.1 Solar Radiation

Total amount of hourly global radiation reaching the tilted surface at any instant is given by (Sukhatme, 1984)

$$I_o = I_b R_b + I_d R_d + (I_b + I_d) R_r \quad (2. 1)$$

where,

I_b : hourly beam radiation

I_d : hourly diffuse radiation

R_b : tilt factor for beam radiation

$$= \frac{\cos \theta}{\cos \theta_z}$$

R_d : tilt factor for diffuse radiation

$$= \frac{1 + \cos \beta}{2}$$

R_r : tilt factor for reflected radiation

$$= \rho \left(\frac{1 + \cos \beta}{2} \right)$$

Now,

$$I_b = I_{bn} \cos \theta_z$$

According to **ASHRAE model**, for a clear (cloudless) day

$$I_{bn} = A \exp\left(-\frac{B}{\cos \theta_z}\right)$$

$$I_d = CI_{bn}$$

where,

I_{bn} : beam radiation in the direction of the rays

θ_z : angle of incidence on a horizontal surface, i.e. zenith angle

A,B,C are constants whose values have been determined by Threlkald and Jordan(1958).

Total amount of heat flux absorbed by the absorber plate is given by

$$S = I_b R_b (\tau\alpha)_b + ((I_d R_d) + (I_b + I_d)) R_r (\tau\alpha)_d \quad (2. 2)$$

where,

$(\tau\alpha)_b$: transmissivity-absorptivity product for constant radiation

$(\tau\alpha)_d$: transmissivity- absorptivity product for diffuse radiation

2.2 Governing Equations for the multidimensional and Transient Analysis

This section provides a more appropriate and accurate multidimensional-transient approach for the analysis of a liquid flat plate solar collector. The mathematical description of the multidimensional-transient phenomena in the different collector zones is presented here. Properties of the fluid and the materials have been considered to be independent of temperature and invariant with time. Depending on the relative values of the different dimensions, thermal energy transfer through the solid zones have been considered to be two or three dimensional e.g. the heat exchange through the insulation has been considered to be three dimensional while that through the plate has been considered to be two dimensional. Temperature variation of the fluid flowing inside the ducts is taken as one dimensional in the flow direction. Finally, the free convection in the air gap zone, i.e., between the absorber plate and the flat plate collector cover is taken into account by means of an empirical expression suggested by Buchberg et al. (1976).

2.2.1 Cover

The cover thickness is so small that it is reasonable to consider a uniform temperature through it. Hence, we get a two dimensional distribution of temperature, $T_c(x, y)$, in the cover. The governing equation can be obtained from an energy balance in a small volume of thickness, δ_c , of the cover as,

$$k_c \left[\frac{\partial^2 T_c}{\partial x^2} + \frac{\partial^2 T_c}{\partial y^2} \right] + \frac{q_{p-c}}{\delta_c} + \frac{q_{a-c}}{\delta_c} + q_{abs} = \rho_c C_c \frac{\partial T_c}{\partial t} \quad (2.3)$$

where,

- ρ_c : density of the cover
- C_c : specific heat of the cover
- k_c : thermal conductivity of the cover
- q_{p-c} : heat flux from absorber plate to the cover
 = average convective heat flux (from absorber plate to cover) +
 average radiative heat flux (from absorber plate to cover)
 = $h_{p-c}(T_{pm} - T_{cm}) + \frac{\sigma(T_{pm}^4 - T_{cm}^4)}{(\frac{1}{\epsilon_p} + \frac{1}{\epsilon_c} - 1)}$
- q_{a-c} : heat flux from ambient to the cover
 = convective heat flux (from ambient to cover) +
 radiative heat flux (from ambient to cover)
 = $h_w(T_a - T_c) + \sigma\epsilon_c(T_{sky}^4 - T_c^4)$
- q_{abs} : heat absorbed by the cover per unit volume
 = $I_o \frac{[1 - \exp(-\frac{K\delta_c}{\cos\theta_2})]}{\delta_c}$

The symbols $T_a, T_{pm}, T_{cm}, \epsilon_p, \epsilon_c, K$ stand for ambient temperature, mean plate temperature, mean cover temperature, emissivity of plate, emissivity of cover and extinction coefficient respectively. The symbol h_{p-c} stands for convective heat transfer coefficient between plate and cover and is obtained by using the empirical expression suggested by Buchberg et al. (1976). An empirical expression for convective heat transfer coefficient between plate and ambient, h_w , has been proposed by McAdams (1954). The heat absorbed by cover, q_{abs} , is calculated using Bouger's law for a partially transparent medium (Duffie and Beckman, 1980).

It may be noted that the thermal radiation term from ambient to cover is calculated considering the ambient air as a black body which emits at sky temperature . The sky temperature is calculated from empirical relation given below (Sukhatme, 1984):

$$T_{sky} = T_{amb} - 6$$

Adiabatic condition is considered on the boundary, i.e.

$$\frac{\partial T_c}{\partial n} = 0 \quad (2.4)$$

2.2.2 Plate

As in the case of the cover, here also we consider a two dimensional variation in the temperature of the absorber plate i.e. $T_p(x, y)$. The governing energy equation can be obtained, as before, by a heat balance on an element of thickness, δ_p , of the plate as,

$$k_p \left(\frac{\partial^2 T_p}{\partial x^2} + \frac{\partial^2 T_p}{\partial y^2} \right) + \frac{q_{f-p}}{\delta_p} + \frac{q_{i-p}}{\delta_p} + \frac{q_{c-p}}{\delta_p} + \frac{S}{\delta_p} = \rho_p C_p \frac{\partial T_p}{\partial t} \quad (2.5)$$

where,

- ρ_p : density of the absorber plate
- C_p : specific heat of the absorber plate
- k_p : thermal conductivity of the absorber plate
- S : solar flux absorbed by the absorber plate
- q_{f-p} : heat flux from fluid to absorber plate
 $= h_f(T_f - T_p)$
- q_{i-p} : heat flux from insulation to absorber plate
 $= -k_i \frac{\partial T_i}{\partial z} \big|_{z=\delta_i}$
- q_{c-p} : heat flux from cover to absorber plate
 $= h_{p-c}(T_{cm} - T_{pm}) + \frac{\sigma(T_{cm}^4 - T_{pm}^4)}{(\frac{1}{\epsilon_c} + \frac{1}{\epsilon_p} - 1)}$

Heat transfer coefficient between plate and fluid, h_f , is calculated using the assumption that heat transfer from plate to fluid takes place under ‘constant heat flux’ condition (Wong, 1977).

Adiabatic condition is considered on the boundary, i.e.

$$\frac{\partial T_p}{\partial n} = 0 \quad (2. 6)$$

2.2.3 Insulation

The temperature distribution $T_i(x, y, z)$ in the insulation is considered to be three dimensional. The governing energy equation is written as :

$$k_i \left(\frac{\partial^2 T_i}{\partial x^2} + \frac{\partial^2 T_i}{\partial y^2} + \frac{\partial^2 T_i}{\partial z^2} \right) = \rho_i C_i \frac{\partial T_i}{\partial t} \quad (2. 7)$$

where,

ρ_i : density of the insulation

C_i : specific heat of the insulation

k_i : thermal conductivity of the insulation

There is no heat generation or absorption inside the insulation. The boundary conditions are:

- Faces exposed to the atmosphere

$$-k_i \left(\frac{\partial T_i}{\partial n} \right) = h_w (T_i - T_a) \quad (2. 8)$$

- Face in contact with the absorber plate

$$T_i = T_p \quad (2. 9)$$

2.2.4 Fluid

The fluid flow in the duct is considered to be one dimensional i.e. average values of temperature, $T_f(y)$, are used in each cross sectional area of the fluid stream. The governing energy equation of the fluid flow is:

$$q_{p-f}.R - \frac{\dot{m}}{N}C_f \frac{\partial T_f}{\partial y} = \rho_f A_f C_f \frac{\partial T_f}{\partial t} \quad (2. 10)$$

where,

- ρ_f : density of the fluid
- C_f : specific heat of the fluid
- \dot{m} : mass flow rate of the fluid
- N : number of ducts
- q_{p-f} : convective heat flux from the absorber plate to the fluid
 $= h_f(T_p - T_f)$
- R : πD_i
- A_f : $(\frac{\pi}{4})D_i^2$

The inlet boundary condition for the fluid is

$$\text{at } y = 0 \quad T_f = T_{fi}$$

2.3 Efficiency of a Flat Plate Solar Collector

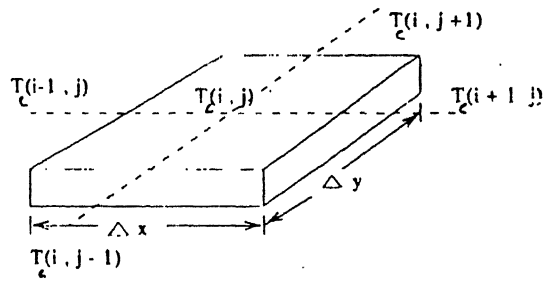
Efficiency is an important parameter to estimate the performance of a collector. The instantaneous efficiency of a flat plate solar collector is defined as the rate of useful heat gain and the flux incident on the collector. The mean efficiency of collector is defined as the ratio of total useful heat gain and the total incident radiation on the collector over the period of its operation.

Chapter 3

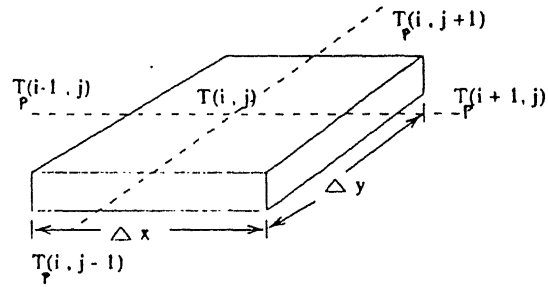
Numerical Modelling

In this chapter, the methods and the discretized equations used in different collector zones are presented. These zones are the cover, insulation, fluid and the absorber plate. The discretized elements of cover, plate, fluid and insulation are shown in Figure 3.1. The grids are so chosen that corresponding $(i, j)^{th}$ coordinates are coincident. The global algorithm for the coupling solution is indicated by a flowchart (Fig3.2). Implicit finite difference method is used for the solution of the various equations. In the method, the entire region is divided into small grids of finite size. Temperatures are calculated on all the nodal points at each time step as we move forward in time domain. In the nomenclature used, i, j and k represent parameters in x, y and z directions respectively and n is the parameter in time domain. Partial derivatives are expressed in the following forms:

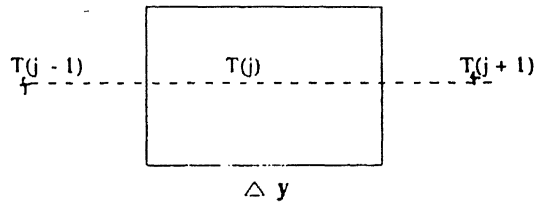
$$\begin{aligned}\frac{\partial T}{\partial x} &= \frac{T_{i+1} - T_{i-1}}{2\Delta x} \\ \frac{\partial^2 T}{\partial x^2} &= \frac{T_{i+1} - 2T_i + T_{i-1}}{\Delta x^2} \\ \frac{\partial T}{\partial t} &= \frac{T^{n+1} - T^n}{\Delta t}\end{aligned}$$



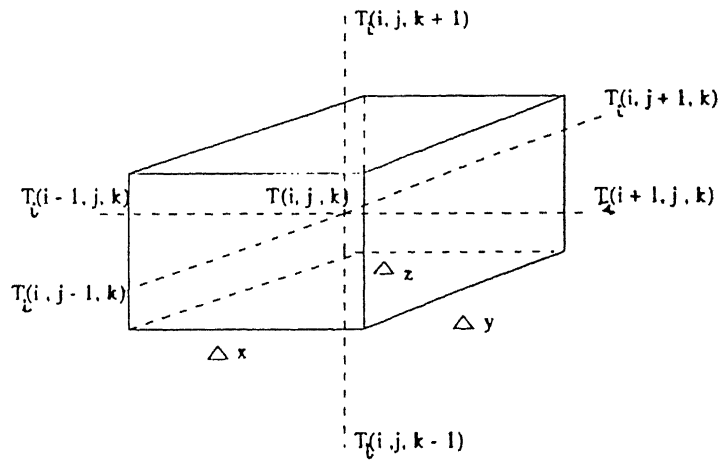
(a) Discrete elements in the cover



(b) Discrete element in the plate



(c) Discrete element in the fluid



(d) Discrete element in the insulation

Figure 3.1 : Discrete elements of different components

3.1 Cover

A set of discretized equations is obtained by numerical approximation of the governing equation(2.3) and its boundary condition(2.4) into each one of the control volumes of the grid. The evaluation of the heat conducted is made using Alternative Direction Implicit (ADI) technique. The convection heat exchanged with outside is taken implicitly and remaining heat exchanges are taken explicitly.

The Boundary Conditions in discretized form can be expressed as

at

$$\begin{aligned} i &= 1 & T_c(i-1, j) &= T_c(i+1, j) \\ j &= 1 & T_c(i, j-1) &= T_c(i, j+1) \\ i &= n_x & T_c(i+1, j) &= T_c(i-1, j) \\ j &= n_y & T_c(i, j+1) &= T_c(i, j-1) \end{aligned}$$

Two equations are established for each point of the grid, each one implicit in one direction.

(1) First equation in which the conduction is evaluated implicitly in the x direction:

$$pT_c(i-1, j, n+1/2) + qT_c(i, j, n+1/2) + rT_c(i+1, j, n+1/2) = s \quad (3.1)$$

where,

$$\begin{aligned} p &= k_c \Delta y \frac{\delta_c}{\Delta x} \\ q &= -[2k_c \Delta y \frac{\delta_c}{\Delta x} + 2\rho_c C_c \Delta x \Delta y \frac{\delta_c}{\Delta t} + h_w \Delta x \Delta y] \\ r &= k_c \Delta y \frac{\delta_c}{\Delta x} \\ s &= -k_c \Delta x \frac{\delta_c}{\Delta y} [T_c(i, j-1, n) - 2T_c(i, j, n) + T_c(i, j+1, n)] - \Delta x \Delta y [h_{p-c} \\ &\quad (T_{pm} - T_{cm}) + \frac{\sigma(T_{pm}^4 - T_{cm}^4)}{(\frac{1}{\epsilon_p} + \frac{1}{\epsilon_c} - 1)}] - \Delta x \Delta y [h_w T_{amb} + \sigma \epsilon_c (T_{sky}^4 - T_c^4(i, j, n))] \\ &\quad - q_{abs} \Delta x \Delta y \delta_c - 2\rho_c C_c \Delta x \Delta y \delta_c \frac{T_c(i, j, n)}{\Delta t} \end{aligned}$$

(2) second equation in which the conduction is evaluated implicitly in the y direction:

$$pT_c(i, j-1, n+1) + qT_c(i, j, n+1) + rT_c(i, j+1, n+1) = s \quad (3.2)$$

where,

$$\begin{aligned} p &= k_c \Delta x \frac{\delta_c}{\Delta y} \\ q &= -[2k_c \Delta x \frac{\delta_c}{\Delta y} + 2\rho_c C_c \Delta x \Delta y \frac{\delta_c}{\Delta t} + h_w \Delta x \Delta y] \\ r &= k_c \Delta x \frac{\delta_c}{\Delta y} \\ s &= -k_c \Delta y \frac{\delta_c}{\Delta x} [T_c(i-1, j, n+1/2) - 2T_c(i, j, n+1/2) + T_c(i+1, j, n+1/2)] - \\ &\quad \Delta x \Delta y [h_{p-c}(T_{pm} - T_{cm}) + \frac{\sigma(T_{pm}^4 - T_{cm}^4)}{(\frac{1}{\epsilon_p} + \frac{1}{\epsilon_c} - 1)}] - \Delta x \Delta y [h_w T_a + \sigma \epsilon_c (T_{sky}^4 \\ &\quad - T_c^4(i, j, n+1/2))] - q_{abs} \Delta x \Delta y \delta_c - 2\rho_c C_c \Delta x \Delta y \delta_c \frac{T_c(i, j, n+1/2)}{\Delta t} \end{aligned}$$

The coefficient matrices of the resultant equations 3.1 and 3.2 are tridiagonal and, therefore, can be solved by a Tridiagonal Matrix Algorithm (Thomas, 1994).

3.2 Plate

The governing energy equation for absorber plate is (2.5). A discretized equation is obtained by numerical approximation of the governing equation, using ADI criteria. Heat exchanges on cover side and with fluid and insulation are calculated explicitly.

The Boundary conditions are

at

$$\begin{aligned} i &= 1 & T_p(i-1, j) &= T_p(i+1, j) \\ j &= 1 & T_p(i, j-1) &= T_p(i, j+1) \\ i &= n_x & T_p(i+1, j) &= T_p(i-1, j) \\ j &= n_y & T_p(i, j+1) &= T_p(i, j-1) \end{aligned}$$

Two equations are obtained for each point of the grid, each one implicit in one direction.

(1) First implicit equation in x direction

$$pT_p(i-1, j, n+1/2) + qT_p(i, j, n+1/2) + rT_p(i+1, j, n+1/2) = s \quad (3.3)$$

where,

$$\begin{aligned} p &= k_p \Delta y \frac{\delta_p}{\Delta x} \\ q &= -[2k_p \Delta y \frac{\delta_p}{\Delta x} + 2\rho_p C_p \Delta x \Delta y \frac{\delta_p}{\Delta t}] \\ r &= k_p \Delta y \frac{\delta_p}{\Delta x} \\ s &= -k_p \Delta x \frac{\delta_p}{\Delta y} [T_p(i, j-1, n) - 2T_p(i, j, n) + T_p(i, j+1, n)] - h_f R \Delta y \\ &\quad [T_f(i, j, n) - T_p(i, j, n)] + \Delta x \Delta y [h_{p-c}(T_{pm} - T_{cm}) + \frac{\sigma(T_{pm}^4 - T_{cm}^4)}{(\frac{1}{\epsilon_p} + \frac{1}{\epsilon_c} - 1)}] - k_i \frac{\Delta x \Delta y}{\Delta z} \\ &\quad [T_i(i, j, n_z - 1, n) - T_i(i, j, n_z, n)] - S \Delta x \Delta y - 2\rho_p C_p \Delta x \Delta y \delta_p \frac{T_p(i, j, n)}{\Delta t} \end{aligned}$$

(2) Second implicit equation in y direction

$$pT_p(i, j-1, n+1) + qT_p(i, j, n+1) + rT_p(i, j+1, n+1) = s \quad (3.4)$$

where,

$$\begin{aligned} p &= k_p \Delta x \frac{\delta_p}{\Delta y} \\ q &= -[2k_p \Delta x \frac{\delta_p}{\Delta y} + 2\rho_p C_p \Delta x \Delta y \frac{\delta_p}{\Delta t}] \\ r &= k_p \Delta x \frac{\delta_p}{\Delta y} \\ s &= -k_p \Delta y \frac{\delta_p}{\Delta x} [T_p(i-1, j, n+1/2) - 2T_p(i, j, n+1/2) + T_p(i+1, j, n+1/2)] - h_f R \end{aligned}$$

$$\Delta y [T_f(i, j, n) - T_p(i, j, n)] + \Delta x \Delta y [h_{p-c}(T_{pm} - T_{cm}) + \frac{\sigma(T_{pm}^4 - T_{cm}^4)}{(\frac{1}{\epsilon_p} + \frac{1}{\epsilon_c} - 1)}] - k_i \frac{\Delta x \Delta y}{\Delta z} [T_i(i, j, n_z - 1, n) - T_i(i, j, n_z, n)] - S \Delta x \Delta y - 2\rho_p C_p \Delta x \Delta y \delta_p \frac{T_p(i, j, n + 1/2)}{\Delta t}$$

The coefficient matrices of resultant sets of equations are tridiagonal and, therefore, can be solved by a Tridiagonal Matrix Algorithm (TDMA).

3.3 Insulation

The discretization is carried out by means of a regular three dimensional grid. For each one of the control volume elements, a discretized equation is obtained as a result of numerical approximation of the governing equation(2.7) and its boundary condition(2.8 and 2.9). ADI method is used for evaluation of the heat conduction. The boundary conditions are

at

$$\begin{aligned} i &= 1 & T_i(i-1, j, k) &= T_i(i+1, j, k) - 2\frac{h_w \Delta x}{k_i} [T_i(i, j, k) - T_{amb}] \\ j &= 1 & T_i(i, j-1, k) &= T_i(i, j+1, k) - 2\frac{h_w \Delta y}{k_i} [T_i(i, j, k) - T_{amb}] \\ k &= 1 & T_i(i, j, k-1) &= T_i(i, j, k+1) - 2\frac{h_w \Delta z}{k_i} [T_i(i, j, k) - T_{amb}] \\ i &= n_x & T_i(i+1, j, k) &= T_i(i-1, j, k) - 2\frac{h_w \Delta x}{k_i} [T_i(i, j, k) - T_{amb}] \\ j &= n_y & T_i(i, j+1, k) &= T_i(i, j-1, k) - 2\frac{h_w \Delta y}{k_i} [T_i(i, j, k) - T_{amb}] \\ k &= n_z & T_i(i, j, k) &= T_p(i, j) \end{aligned}$$

Three equations are obtained for each point of the grid, each one implicit in one direction.

(1) First implicit equation in x direction (move $\frac{\Delta t}{3}$ forward in time domain)

$$pT_i(i-1, j, k, n+1/3) + qT_i(i, j, k, n+1/3) + rT_i(i+1, j, k, n+1/3) = s \quad (3.5)$$

where,

$$\begin{aligned}
p &= k_i \frac{\Delta y \Delta z}{\Delta x} \\
q &= -[2k_i \frac{\Delta y \Delta z}{\Delta x} + 3\rho_i C_i \frac{\Delta x \Delta y \Delta z}{\Delta t}] \\
r &= k_i \frac{\Delta x \Delta y}{\Delta z} \\
s &= -k_i \frac{\Delta x \Delta z}{\Delta y} [T_i(i, j-1, k, n) - 2T_i(i, j, k, n) + T_i(i, j+1, k, n)] \\
&\quad -k_i \frac{\Delta x \Delta y}{\Delta z} [T_i(i, j, k-1, n) - 2T_i(i, j, k, n) + T_i(i, j, k+1, n)] \\
&\quad -3\rho_i C_i \Delta x \Delta y \Delta z \frac{T_i(i, j, k, n)}{\Delta t}
\end{aligned}$$

(2) Second implicit equation in y direction (move by another $\frac{\Delta t}{3}$ in time domain)

$$pT_i(i, j-1, k, n+2/3) + qT_i(i, j, k, n+2/3) + rT_i(i, j+1, k, n+2/3) = s \quad (3.6)$$

where,

$$\begin{aligned}
p &= k_i \frac{\Delta x \Delta z}{\Delta y} \\
q &= -[2k_i \frac{\Delta x \Delta z}{\Delta y} + 3\rho_i C_i \frac{\Delta x \Delta y \Delta z}{\Delta t}] \\
r &= k_i \frac{\Delta x \Delta y}{\Delta z} \\
s &= -k_i \frac{\Delta y \Delta z}{\Delta x} [T_i(i-1, j, k, n+1/3) - 2T_i(i, j, k, n+1/3) + T_i(i+1, j, k, n+1/3)] \\
&\quad -k_i \frac{\Delta x \Delta y}{\Delta z} [T_i(i, j, k-1, n+1/3) - 2T_i(i, j, k, n+1/3) + T_i(i, j, k+1, n+1/3)] \\
&\quad -3\rho_i C_i \Delta x \Delta y \Delta z \frac{T_i(i, j, k, n+1/3)}{\Delta t}
\end{aligned}$$

(3) Third implicit equation in z direction(move by last $\frac{\Delta t}{3}$ in time domain)

$$pT_i(i, j, k-1, n+1) + qT_i(i, j, k, n+1) + rT_i(i, j, k+1, n+1) = s \quad (3.7)$$

where,

$$\begin{aligned} p &= k_i \frac{\Delta x \Delta y}{\Delta z} \\ q &= -[2k_i \frac{\Delta x \Delta y}{\Delta z} + 3\rho_i C_i \frac{\Delta x \Delta y \Delta z}{\Delta t}] \\ r &= k_i \frac{\Delta x \Delta y}{\Delta z} \\ s &= -k_i \frac{\Delta y \Delta z}{\Delta x} [T_i(i-1, j, k, n+2/3) - 2T_i(i, j, k, n+2/3) + T_i(i+1, j, k, n+2/3)] \\ &\quad - k_i \frac{\Delta x \Delta z}{\Delta y} [T_i(i, j-1, k, n+2/3) - 2T_i(i, j, k, n+2/3) + T_i(i, j+1, k, n+2/3)] \\ &\quad - 3\rho_i C_i \Delta x \Delta y \Delta z \frac{T_i(i, j, k, n+2/3)}{\Delta t} \end{aligned}$$

The matrices corresponding to above sets of equations are tridiagonal. Coupled with boundary conditions, the above set of equations is solved one by one using Tridiagonal Matrix Algorithm (TDMA).

3.4 Fluid

For each one of the finite control volume that result by subdividing the pipe, the discretization equations are obtained by numerical approximation of energy equation (2.10). The internal energy transportation is calculated implicitly.

The boundary condition is

$$\text{at } j = 0 \quad T_f(i, j) = T_{f_i}$$

$$T_f(i, j, n+1) = \frac{[\dot{m}C_f T_f(i, j-1, n+1) + h_f C_f A_f \Delta y \frac{T_f(i, j, n)}{\Delta t} + h_f P \Delta y T_p(i, j)]}{[\dot{m}C_f + \rho_f C_f A_f \frac{\Delta y}{\Delta t} + h_f P \Delta y]} \quad (3.8)$$

Thus we see that solving the above system of equations the temperature distribution in different components of flat plate solar collector viz. cover, plate, insulation, fluid can be found out at time $t + \Delta t$ if we know the temperature distribution at time t . The initial temperature distribution is assumed to be known.

Other Features of the Software

The climatological data like wind speed and ambient temperatures must be provided in the form of data files. The time interval of the data normally of one hour, does not necessarily coincide with the one used in the discretization; this makes it necessary to work with interpolation techniques. The day has been assumed to be cloudless and ASHRAE model is used to postulate hourly beam radiation in the direction of the rays. The initial temperature of the different elements of the collector is taken as the ambient temperature when the calculation is initialized. The accuracy improves when the spatial and temporal discretization densities are increased. The numerical solution tends towards an asymptotic value when finer grids are used. For the discretization used, further increment in the density of discretization does not cause appreciable improvement in the numerical solution.

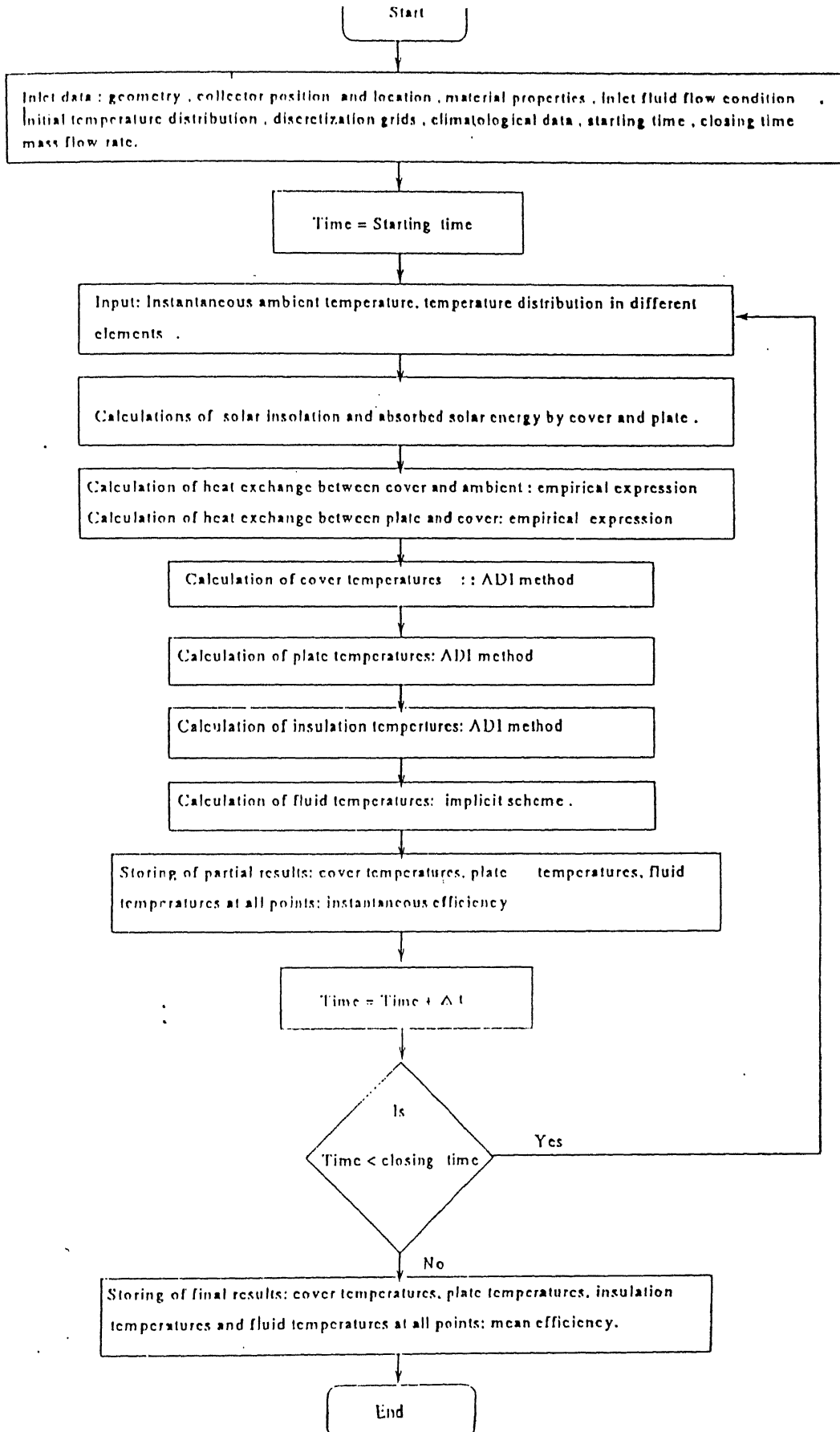


Figure 1. Flow chart of simulation program

Chapter 4

Results and Discussion

4.1 Results

The performance of a flat plate solar collector for a given day, location, position, dimensions and material properties depends on inputs, namely, starting time, closing time, mass flow rate of fluid, inlet fluid temperature and initial temperature distribution in different components of the collector.

The computations in the present analysis have been done for the 21st day of the sixth month (June) of an year at Kanpur (India). The configuration of the collector is same as shown earlier in Figure 1.1. The plate tilt angle for all computations, except the one in which effect of tilt variation is observed, is $24^\circ (0.9\phi)$. The study by Morse and Czarnecki (1958) suggests that for above plate tilt the amount of annual insolation per unit area is maximum. The starting time and closing times have been taken 7:00 hrs and 17:00 hrs respectively. The initial temperature of different elements of flat plate solar collector has been assumed to be equal to that of ambient temperature. The dimensions of collector, material properties and other parameter values used in computation are given in 'Appendix A'.

The variation of ambient temperature and that of incident flux on collector have been shown in Figures 4.1 and 4.2 respectively. Figure 4.3 shows the results of the present analysis and then comparison with available experimental data. It gives the variation of the rise in the fluid temperature with the time of the day. The

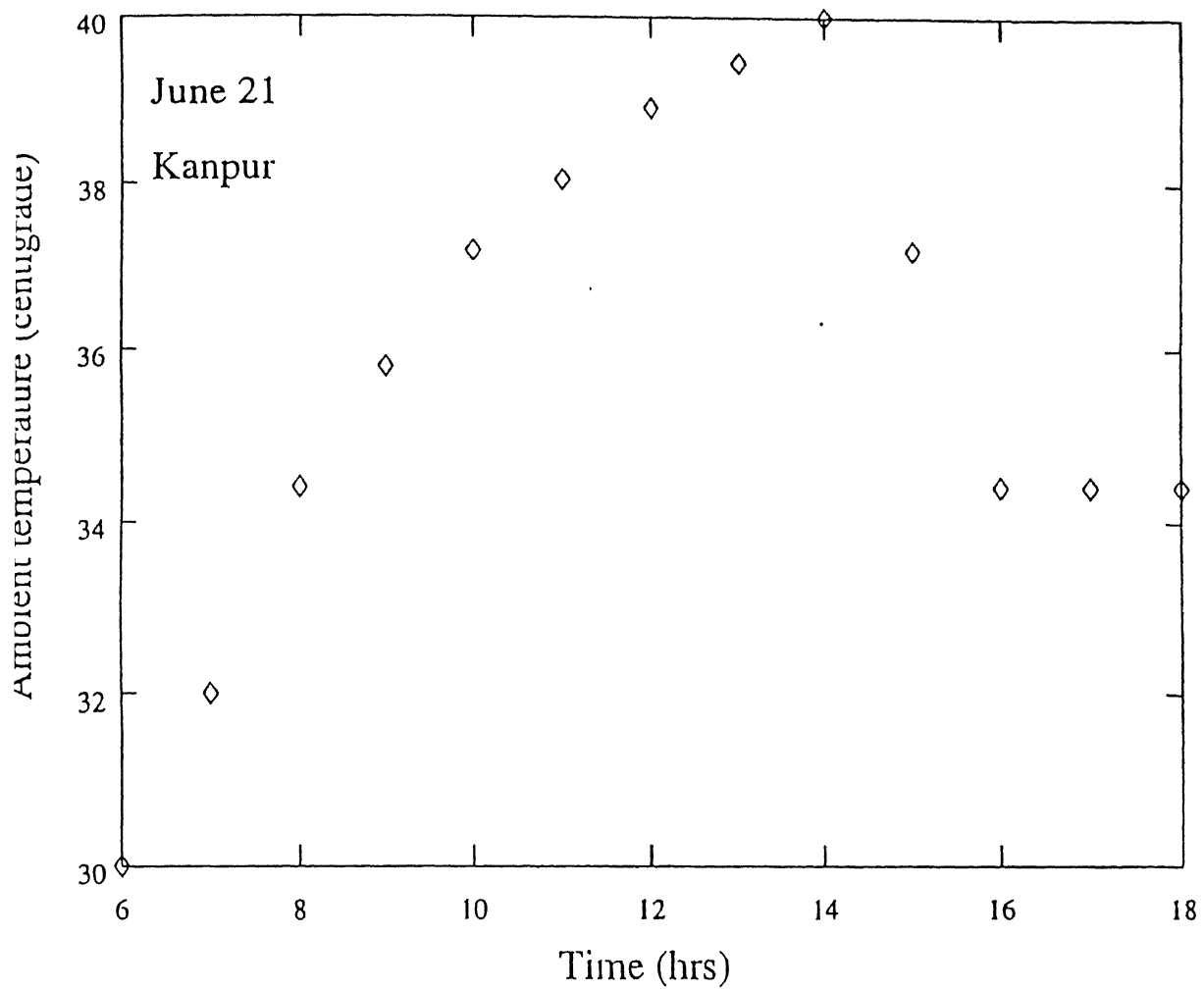


Figure 4.1 : Ambient temperature variation with the time of the day

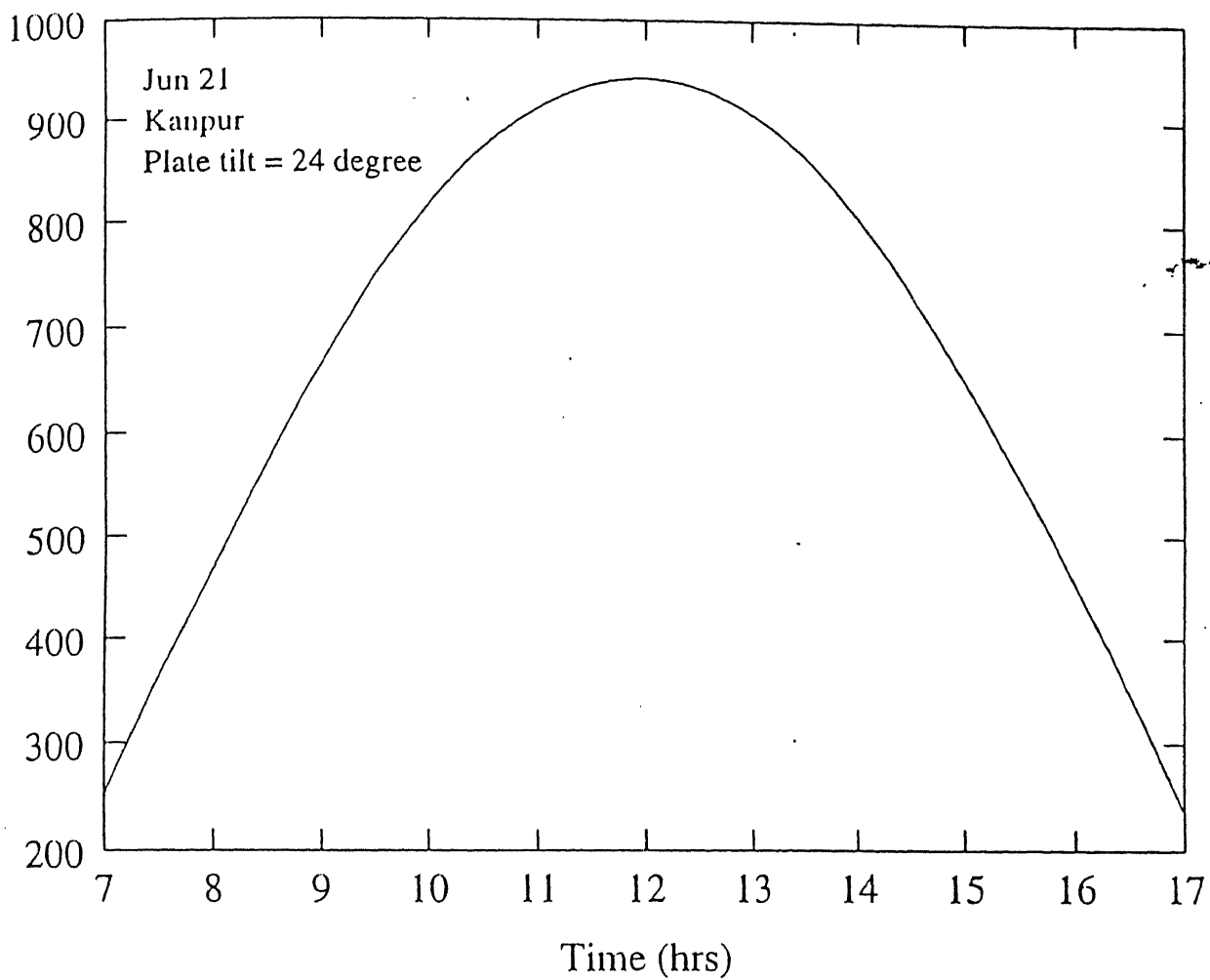


Figure 4.2 : Incident solar flux on collector cover with the time of the day

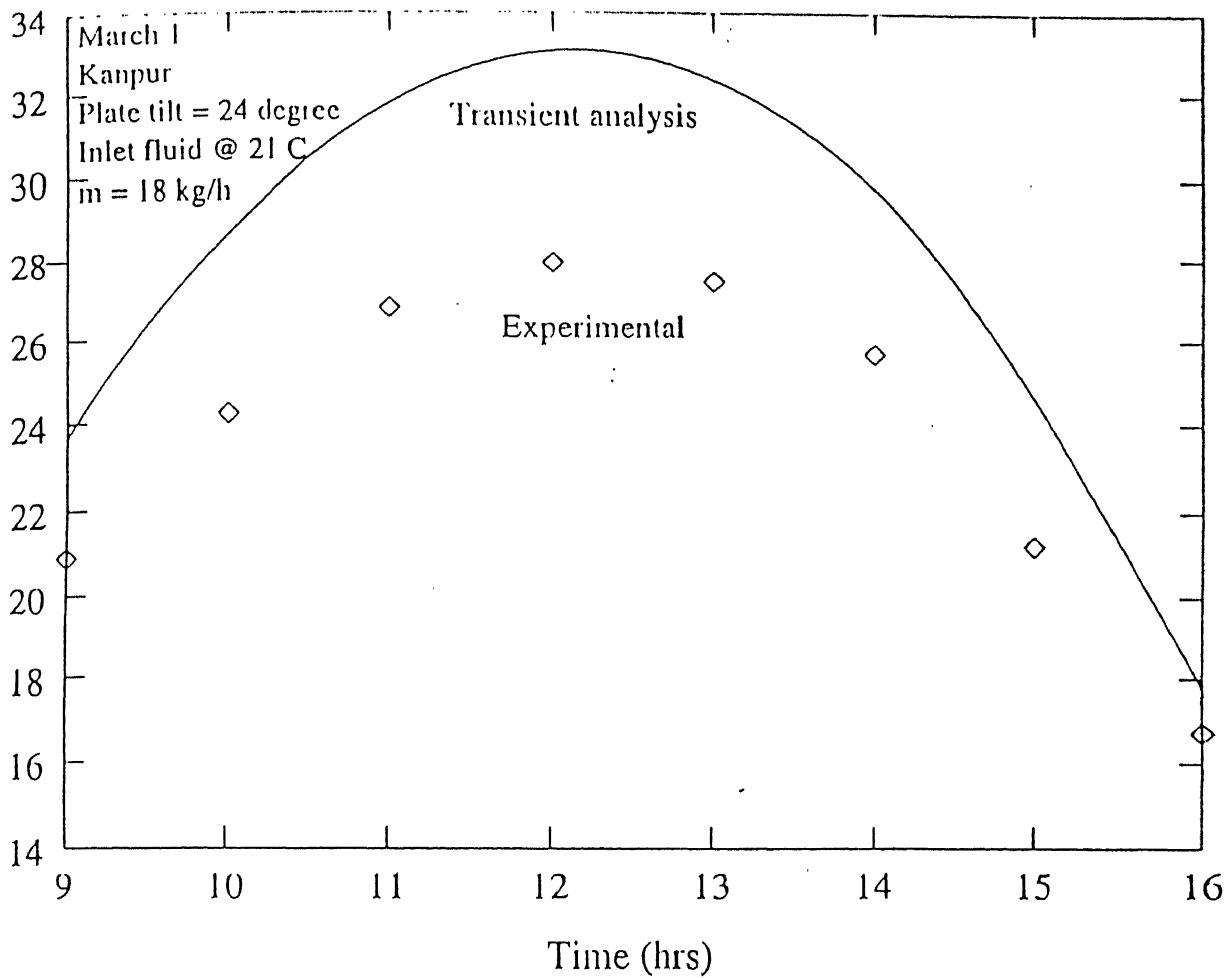


Figure 4.3 : Comparison of the predicted rise in fluid temperature with experimental data

experimental values are from Desai (1985) for 1st of March. To facilitate comparison one set of computations have been done with present multidimensional-transient model for similar inputs. The pattern of rise in fluid temperature with time is similar in both experimental data and that obtained from multidimensional-transient analysis. The peak temperature rise predicted by the present analysis and that from the experimental data occur almost at the same time, the noon. At noon, the rise in fluid temperature, for mass flow rate of 18 kg/h and inlet temperature of 21°C, is 33° C as obtained from multidimensional-transient analysis compared with 28° C of experimental data. The discrepancy between the experimental values and those obtained from multidimensional-transient analysis could be attributed to various factors a few of which are given below :

- (1) the insolation impinging on the plate may be less than the monthly average assumed in the present analysis,
- (2) the wind speed may be higher,
- (3) cover and plate materials may not be of very high quality,
- (4) collector may not be well insulated from the sides.

Figure 4.4 demonstrates the variation of mean plate temperature along the direction of the fluid flow. The plate temperature increases along the direction of the flow because at start, the temperature of fluid is low which increases as it flows through the collector. The variation of mean plate temperature along flow direction has been plotted for three flow rates, namely, 20 kg/h, 60 kg/h and 100 kg/h . As expected, it is observed that the plate temperatures are higher for lower flow rates. This can be explained on account of higher fluid temperatures for lower flow rates.

Figure 4.5 displays the rise in fluid temperatures with time of the day for three different flow rates. The temperature rise first increases till noon and then starts decreasing. It is maximum at about 12 noon, almost at the same time when incident flux is maximum. For mass flow rates of 20 kg/h, 60 kg/h and 100 kg/h, the maximum rise in fluid temperatures are 28°C, 10°C and 6°C respectively.

Figure 4.6 shows the variation of instantaneous efficiency with the time of the day for the three different flow rates, namely, 20 kg/h, 60 kg/h and 100 kg/h. The efficiency rises rapidly from a very small value, at the starting time of 7:00 hrs,

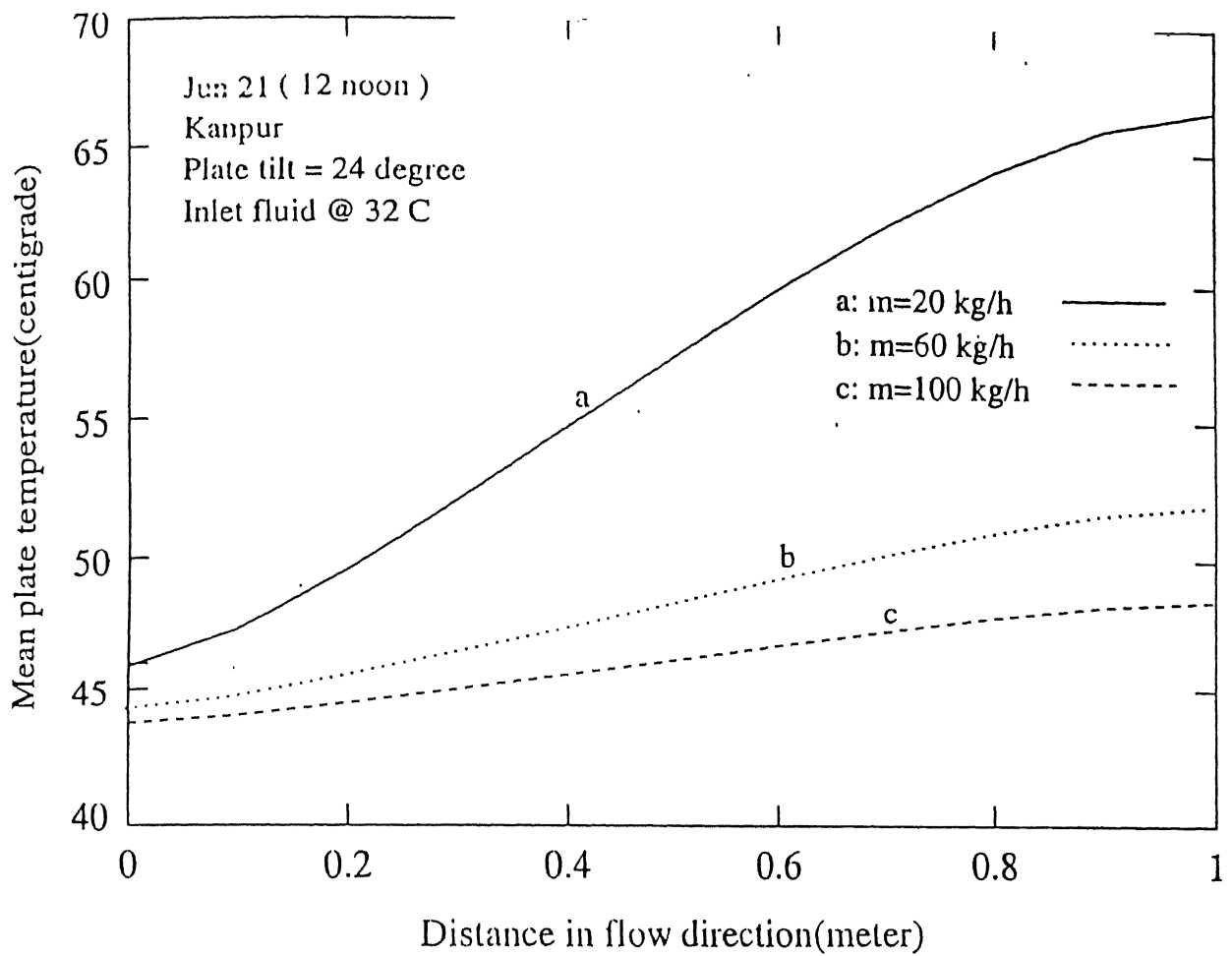


Figure 4.4 : Mean plate temperature along flow direction for different flow rates

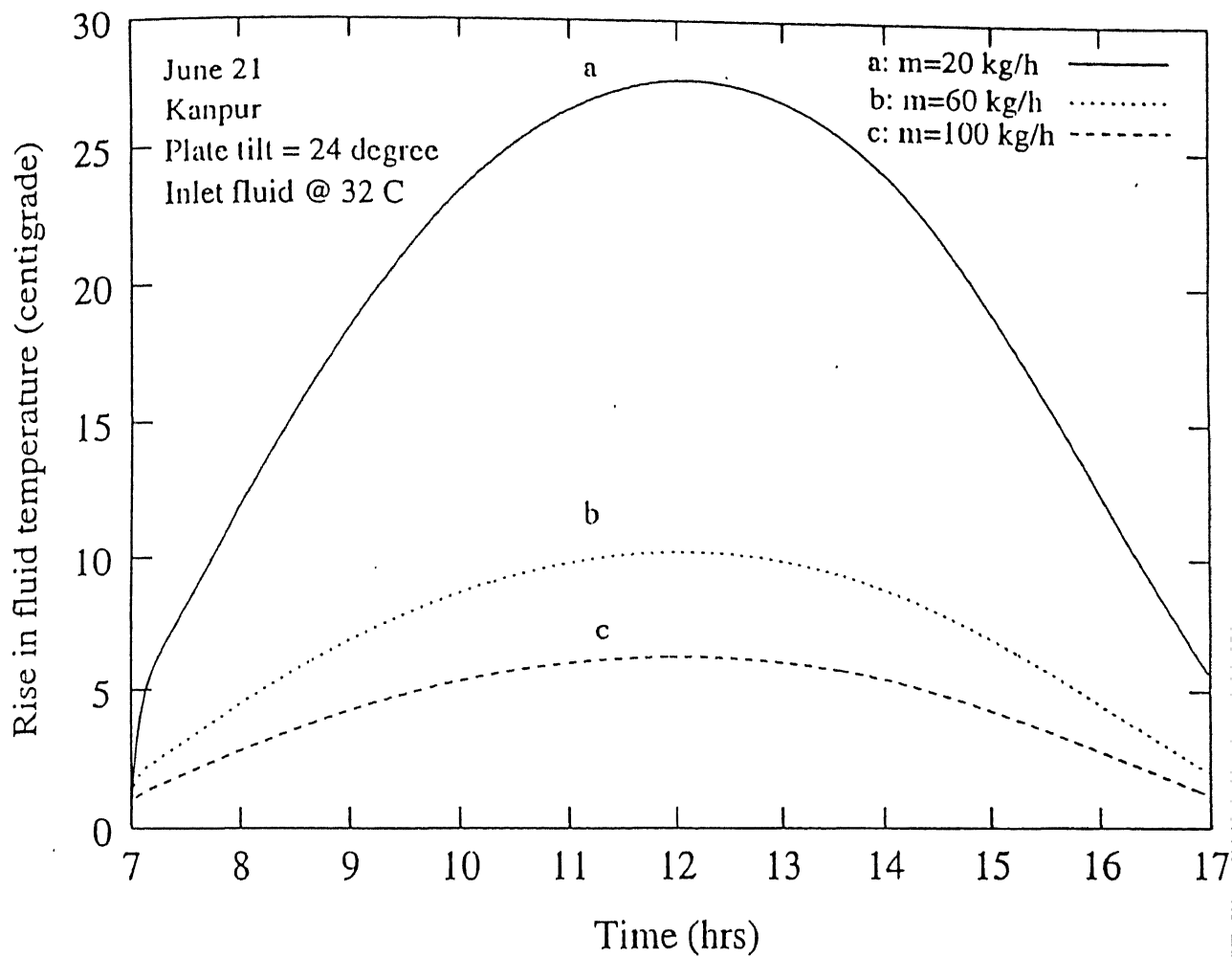


Figure 4.5 : Rise in the fluid temperature with the time of the day for different flow rates

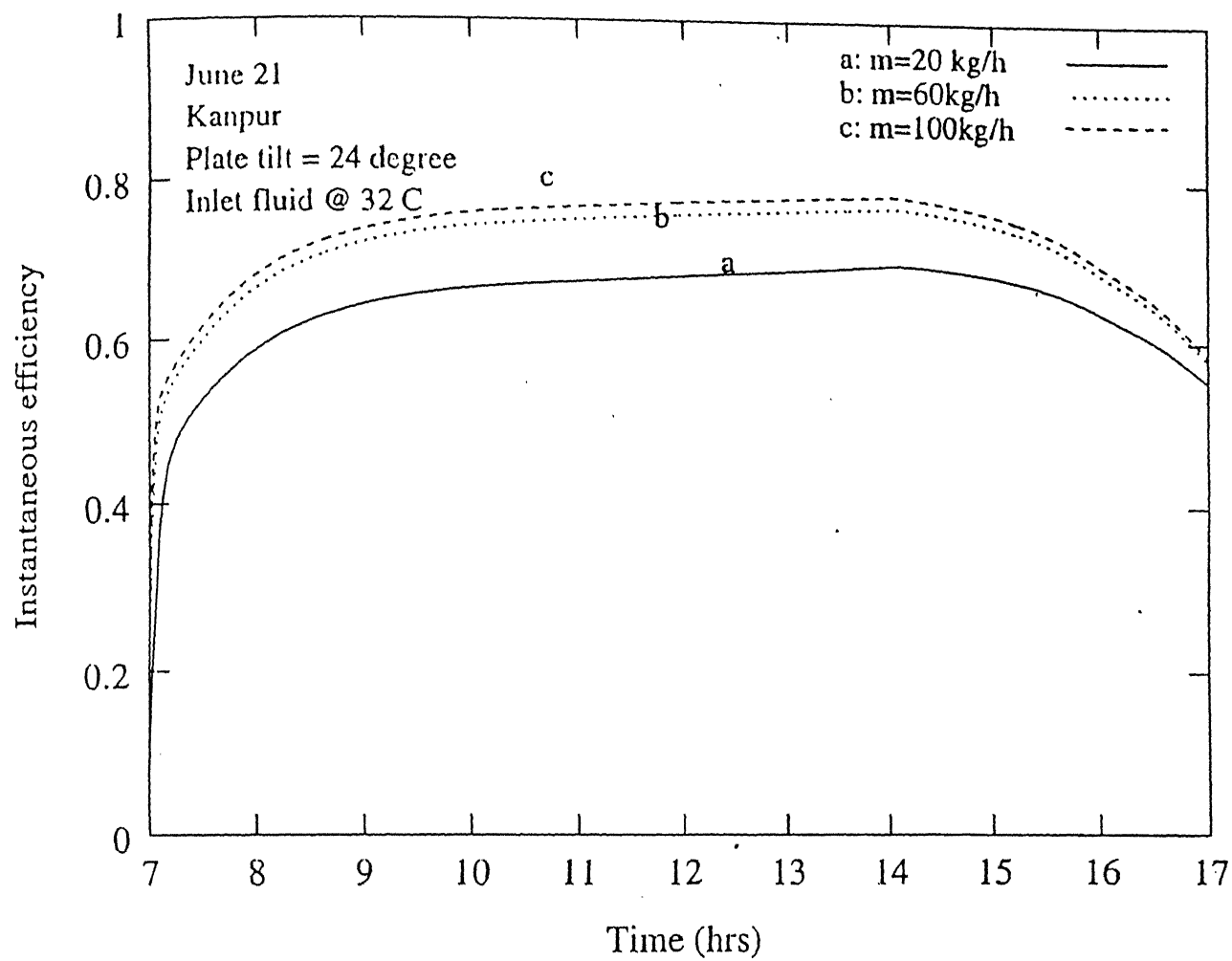


Figure 4.6 : Instantaneous efficiency with the time of the day for different flow rates

till about 10:00 hrs after which it remains nearly constant till about 15:00 hrs and then starts decreasing. This can be explained in following manner. The collector is in transient state during start and much of the incident flux is absorbed by cover, absorber plate and insulation in raising their temperatures before they reach in a quasi-steady state. Thus the useful energy obtained is low during this period and hence the efficiency. From 10:00 hrs till 15:00 hrs, the collector is in a quasi steady state and hence efficiency is nearly constant. After 15:00 hrs the collector efficiency drops rapidly. The results for the period , 10:00 hrs to 15:00 hrs , are in good agreement with the predictions of Agarwal (1996) in his multidimensional-steady analysis. But the results for the periods , 7:00 hrs to 10:00 hrs and 15:00 hrs to 17:00 hrs, diverge from the predictions of Agrawal (1996). This divergence is expected as the transient characteristic of heat transfer are dominant during these periods and the steady state assumption made by Agrawal (1996) is no longer valid for these periods. The pattern of efficiency variation predicted by multidimensional-transient is similar to that predicted by Sukhatme (1984).

Figures 4.7 and 4.8 show the variation of percentage distribution of incident flux with the time of the day for mass flow rates of 20 kg/h and 100 kg/h respectively. The useful energy curve as expected follows exactly the pattern of efficiency curve (see Figure 4.6). The stored energy is positive and significant from 7:00 hrs to 10:00 hrs, implying that transient characteristics are dominant during this period. In the afternoon stored energy becomes negative, implying that the collector components, viz., cover, absorber plate and insulation are dissipating heat instead of absorbing it. From figure 4.8 it is evident that mass for mass flow rate of 100 kg/h during quasi-steady state (i.e. 10:00 hrs to 15:00 hrs) about 75% energy is utilized in heating the fluid, 8% is lost from the top of the cover, 2% is lost from insulation faces and the optical energy loss is 15%.

Figure 4.9 shows the variation of mean efficiency of the collector with mass flow rate. It is observed that efficiency increases as we increase the flow rate from 20 kg/h, but becomes almost constant for flow rates higher than 40 kg/h. For very low flow rates the fluid is not able to carry the heat as fast as the heat is transferred from the plate, this could be one of the reasons for lower efficiency at low flow rates.

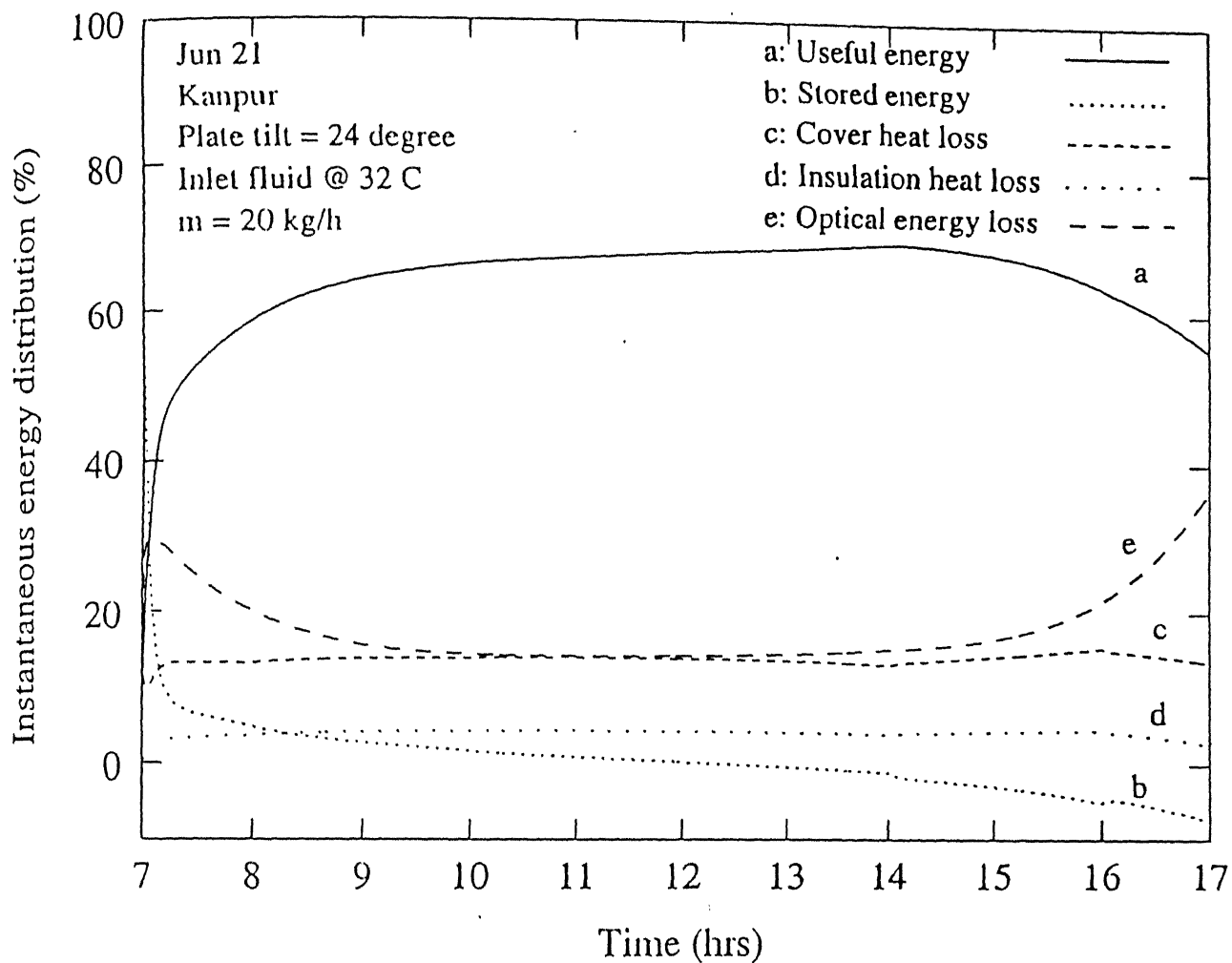


Figure 4.7 : Instantaneous energy distribution with the time of the day

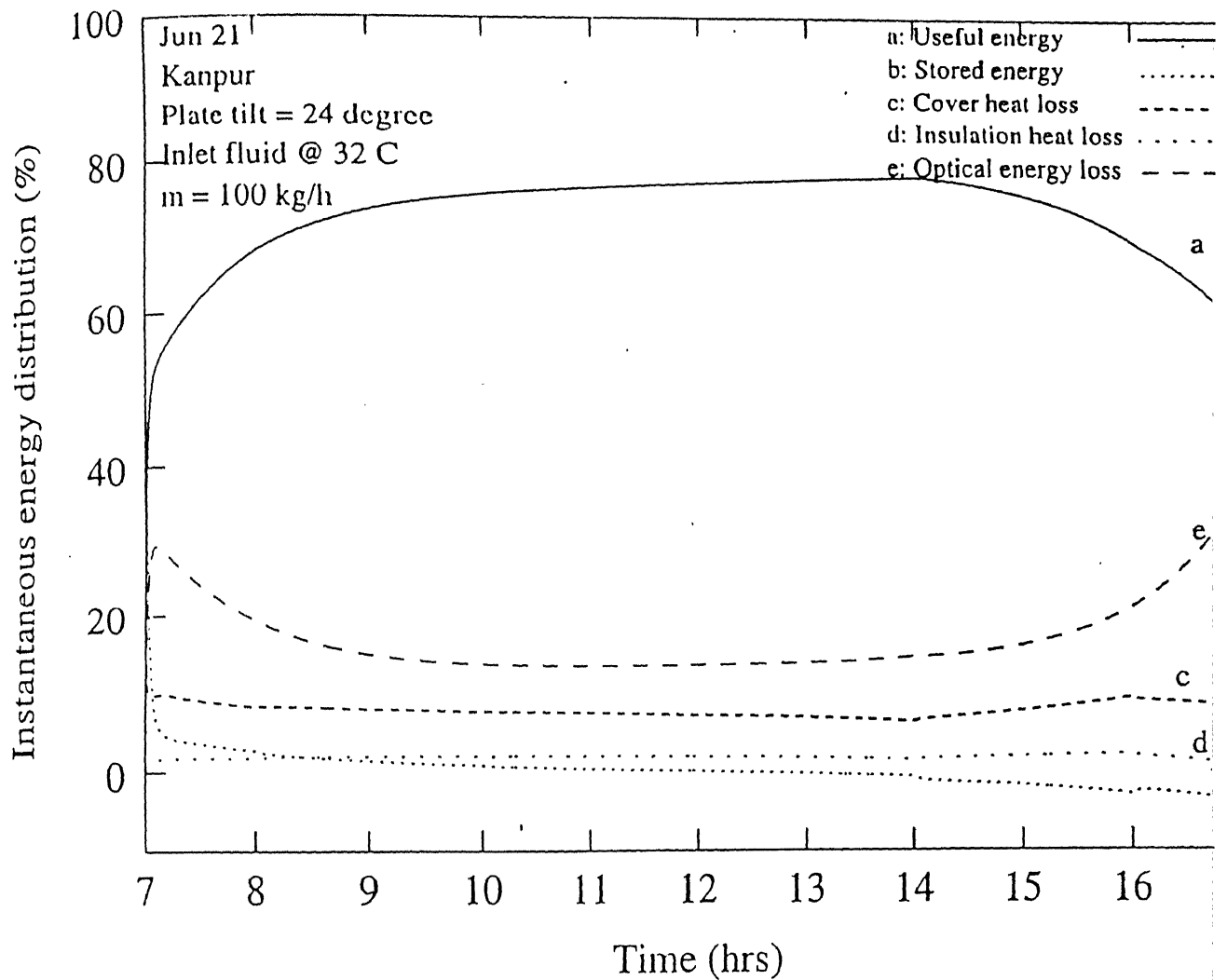


Figure 4.8 : Instantaneous energy distribution with the time of the day

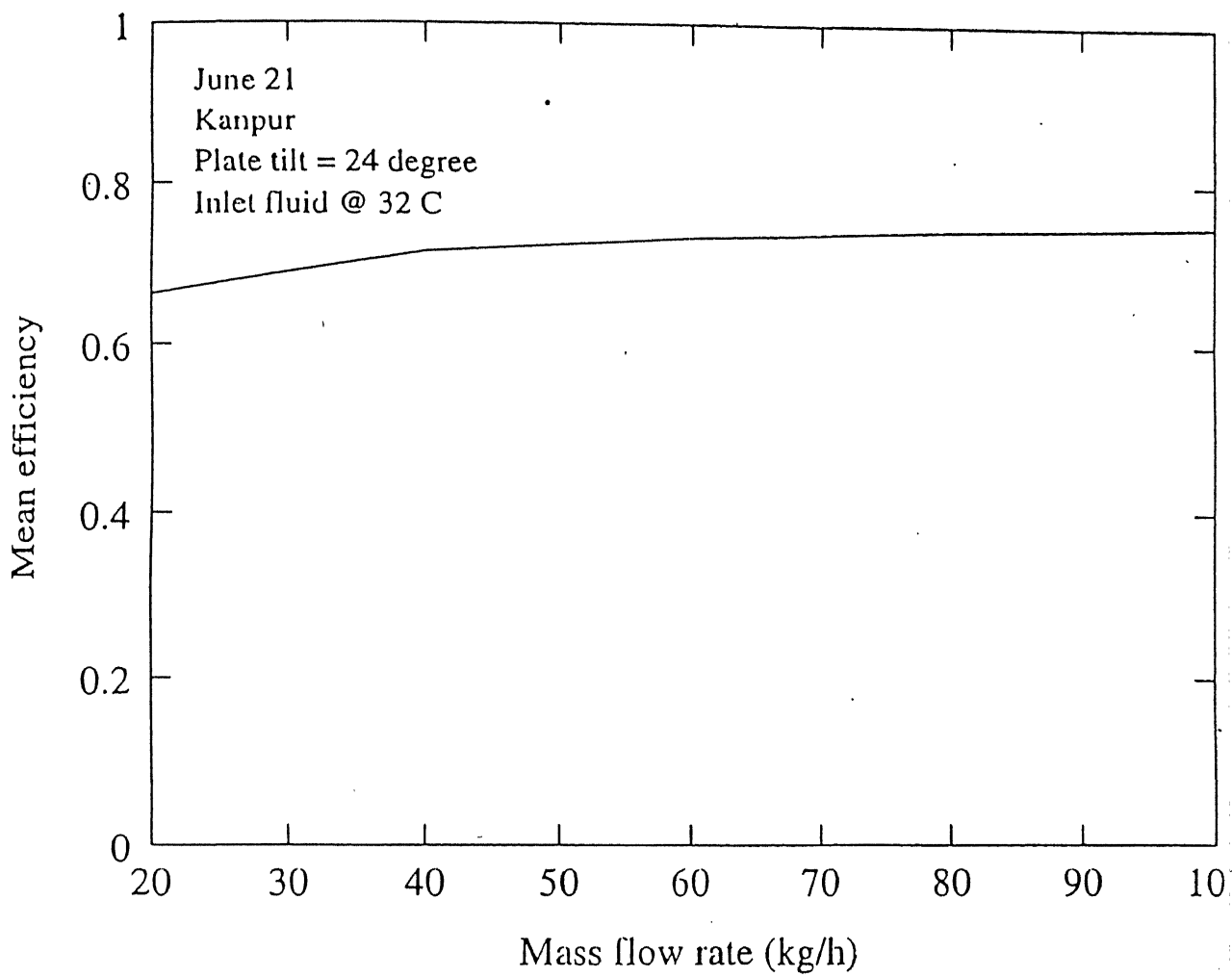


Figure 4.9 : Mean efficiency variation with the flow rate

This further implies that for the optimum utilisation of the flat plate collector the mass flow rate should be greater than 40 kg/h.

As mentioned earlier, a plate tilt of 0.9ϕ gives the maximum insolation per unit area (Morse & Czarnecki, 1958). Infact an optimum tilt is $(\phi - 10^\circ)$ for the summers and $(\phi + 10^\circ)$ for the winters are recommended (Kern & Harris, 1975). The latitude of Kanpur is about 26° . Figures 4.10 and 4.11 show the variation of rise in fluid temperatures with the time of the day for mass flow rates of 20 kg/h and 100 kg/h respectively. Each of the two figures is plotted for three different plate tilt angles, namely, 16° , 24° and 36° . It is observed that rise in fluid temperature is higher for the case of plate tilt of $16^\circ(\phi - 10^\circ)$ and lower for the plate tilt of $36^\circ(\phi + 10^\circ)$ when compared with the case for which plate tilt angle is $24^\circ(0.9\phi)$. The analysis thus, further confirms the claims of Kern and Harris (1975).

The fluid inlet temperature is an important operational parameter which strongly influences the performance of a flat plate solar collector. The effect has been illustrated by plotting the mean collector efficiency with the inlet fluid temperature in Figure 4.12. The inlet fluid temperature varies from $32^\circ C$ to $90^\circ C$. It is observed that efficiency drops sharply at an increasing rate (from 0.64 to 0.13) with increasing inlet fluid temperature (from $32^\circ C$ to $90^\circ C$). These results are in good agreement with those of Sukhatme (1984).

4.2 Conclusion

From the results of the present study, following inferences may be drawn :

- The results of present study are within 15 percent of the available experimental data.
- The collector can be assumed to be in quasi-steady state from 10:00 hrs to 15:00 hrs ,but transient characteristics dominate the performance from 7:00 hrs to 10:00 hrs and 15:00 hrs to 17:00 hrs.
- The rise in fluid temperature is maximum at 12 noon IST for Kanpur (India).

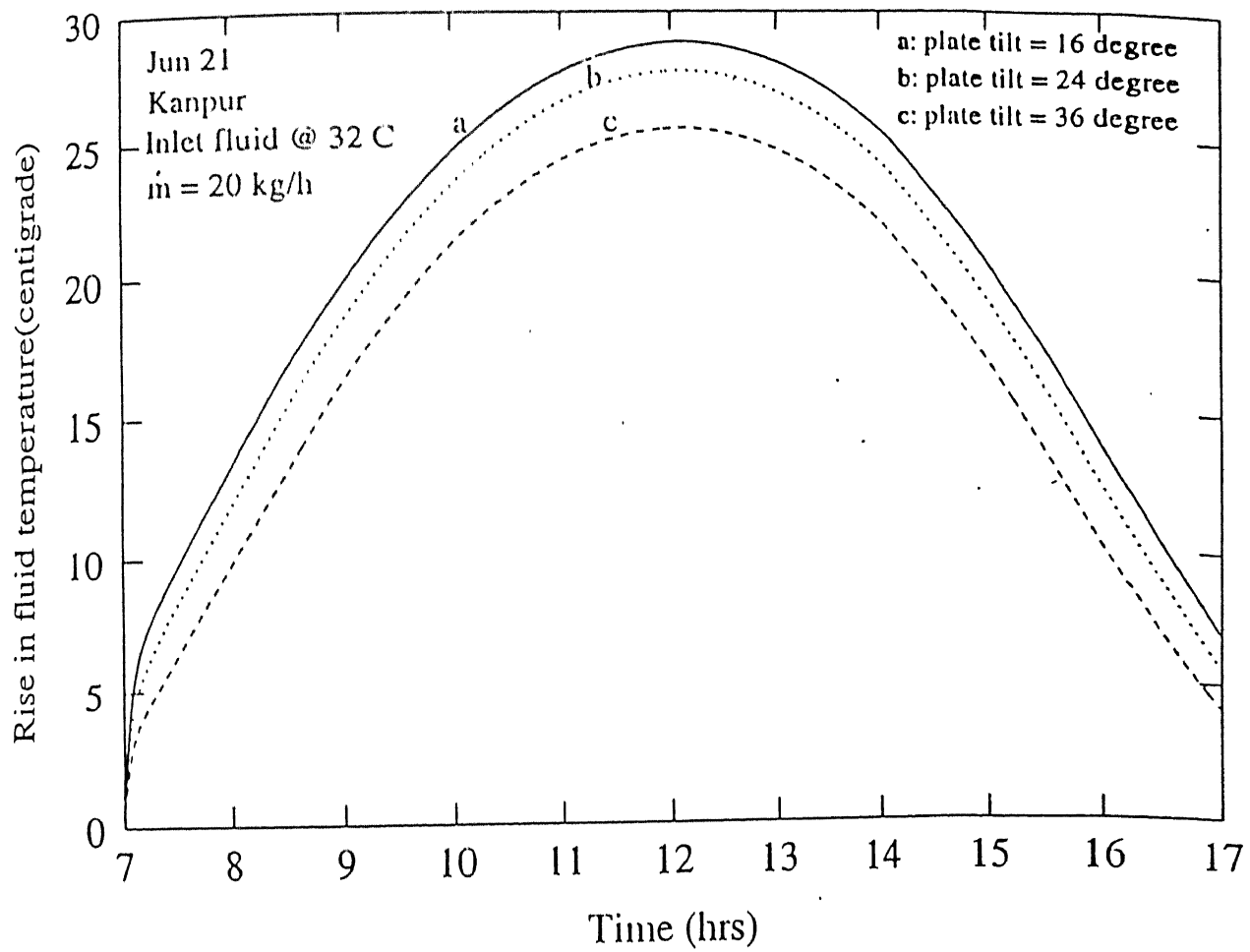


Figure 4.10 : Rise in fluid temperature with time of the day for different tilt angles

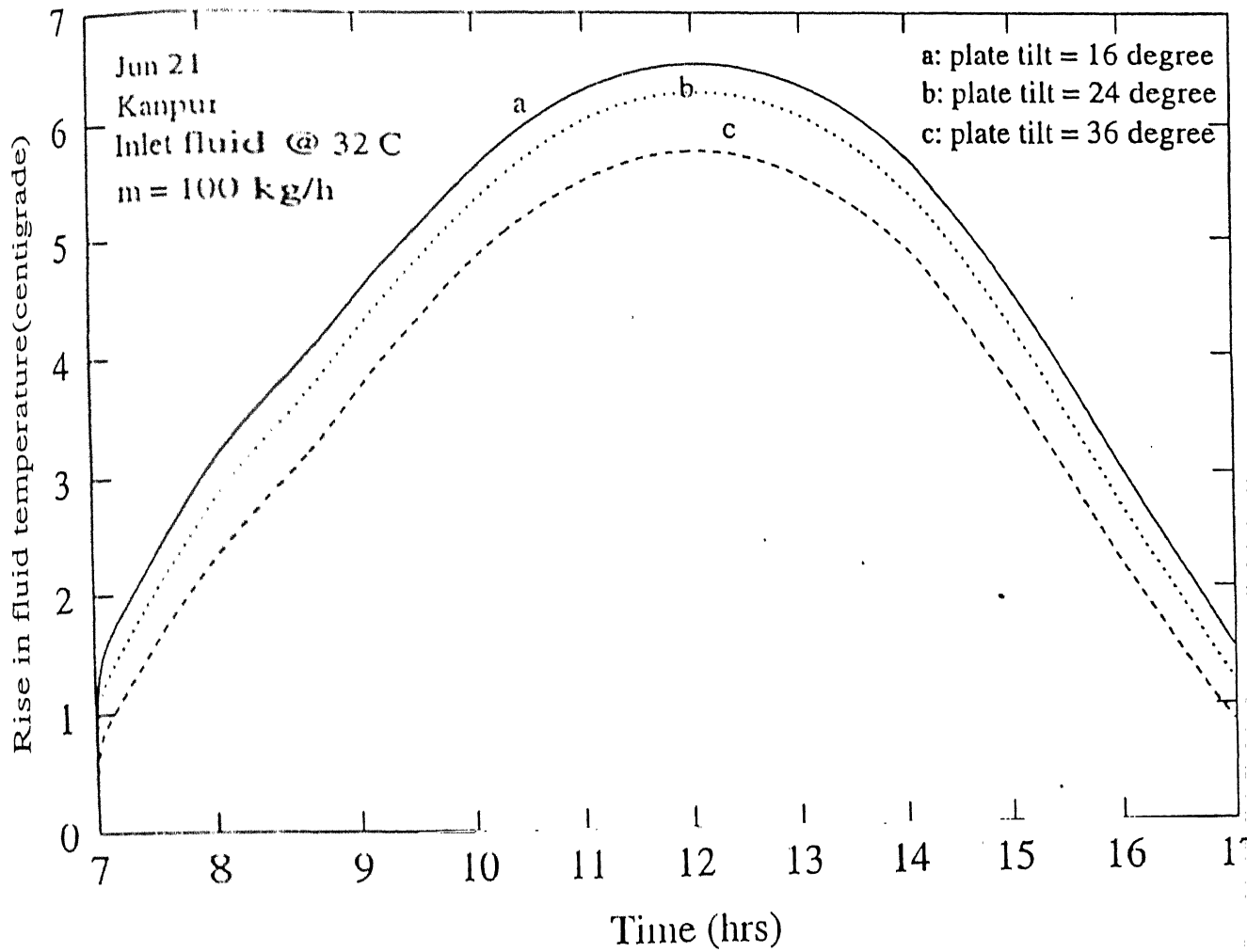


Figure 4.11 : Rise in fluid temperature with time of the day for different tilt angles

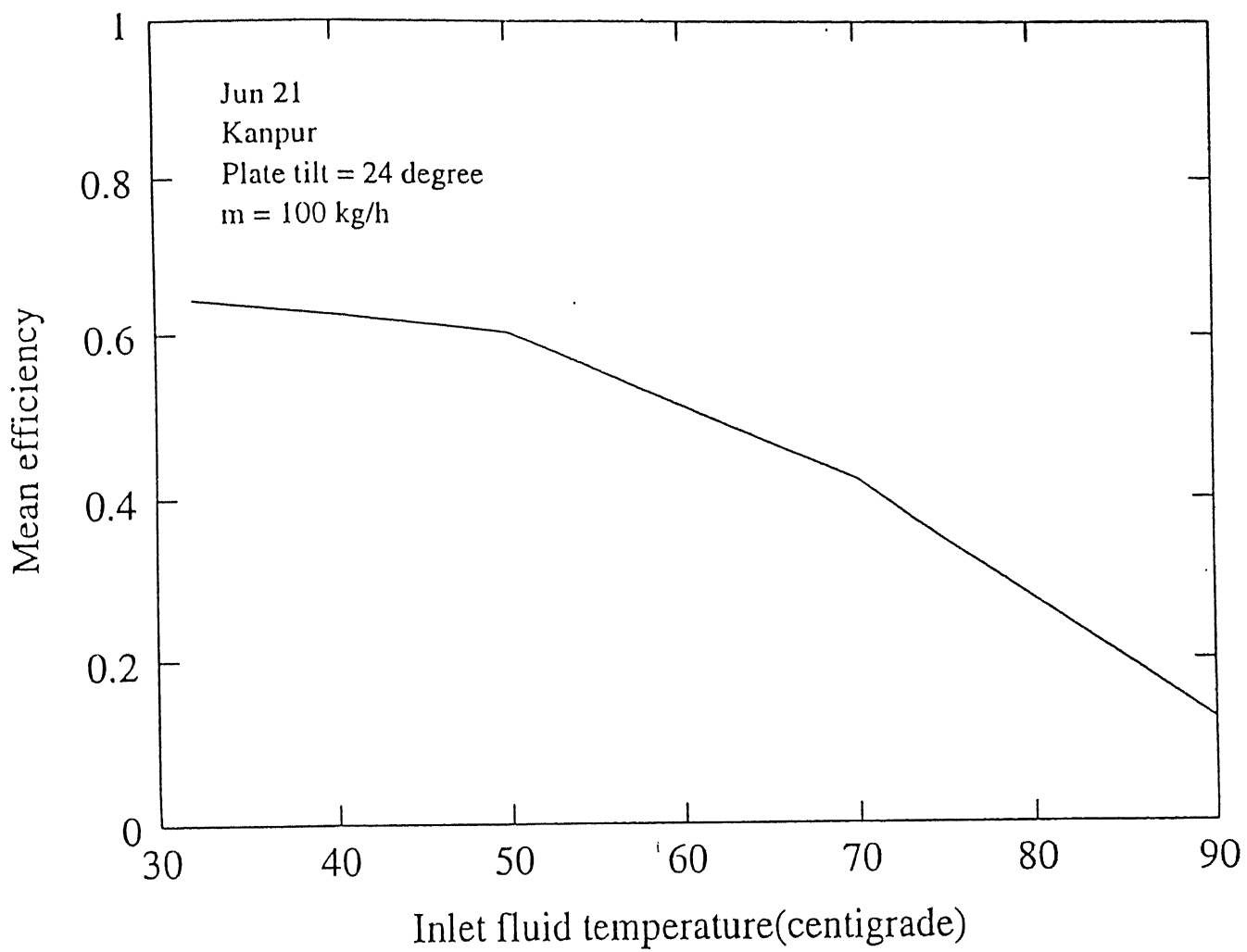


Figure 4.12 : Mean efficiency variation with inlet fluid temperature

- The collector efficiency remains nearly constant for the period from 10:00 hrs to 15:00 hrs.
- Efficiency of the collector increases with flow rate upto 40 kg/h beyond which it remains nearly constant in the laminar flow region.
- Efficiency of collector decreases with increase in inlet fluid temperature.
- In summers a tilt angle of $\phi + 10^\circ$ gives the best performance.

The results discussed in the previous sections are intended to illustrate the possibilities and the versatility of the analysis carried out. There are a host of other parameters like material properties, day of the year, dimension of the collector etc. the effect of which can be studied and optimized with the software developed in the present work. The numerical model presented here which simulates a flat plate solar collector has been shown to be a powerful tool in the analysis of the thermal performance of a collector. With this software depending on requirement, it is possible to make a comprehensive test because it takes into account the multidimensional and transitory aspects that characterize a collector.

4.3 Suggestions for future work

- Experimental verification of the theoretical results presented in the thesis here.
- Incorporation of the variation of physical properties with temperature of the materials involved.
- The effect of shadow, number of covers and dust on top of the collector needs to be investigated.
- The similar multidimensional-transient analysis can be taken up for some of the novel designs like honey comb collector, double exposure collector and the thermal trap collector.

Appendix A

The values of the parameters used are listed below :

Dimension of the collector

| | |
|---|------|
| Width of plate | 1 m |
| Length of Plate | 2 m |
| Thickness of the glass cover (δ_c) | 2 mm |
| Thickness of absorber plate (δ_p) | 2 mm |
| Thickness of insulation (δ_i) | 7 cm |
| Dia of pipe (D) | 1 cm |

Material properties of the collector

| | |
|---|--|
| Thermal conductivity of the glass cover (k_c) | $1.4 \text{ W.m}^{-1}.\text{K}^{-1}$ |
| Thermal conductivity of the copper absorber plate (k_p) | $372 \text{ W.m}^{-1}.\text{K}^{-1}$ |
| Thermal conductivity of the glass wool insulation (k_i) | $0.03 \text{ W.m}^{-1}.\text{K}^{-1}$ |
| Thermal conductivity of the fluid(water) (k_f) | $0.61 \text{ W.m}^{-1}.\text{K}^{-1}$ |
| Specific heat of the glass cover (C_c) | $750 \text{ J.kg}^{-1}.\text{K}^{-1}$ |
| Specific heat of the absorber plate (C_p) | $419 \text{ J.kg}^{-1}.\text{K}^{-1}$ |
| Specific heat of the insulation (C_i) | $836 \text{ J.kg}^{-1}.\text{K}^{-1}$ |
| Specific heat of the fluid (C_f) | $4187 \text{ J.kg}^{-1}.\text{K}^{-1}$ |
| Density of the glass cover (ρ_c) | 2225 kg.m^{-3} |
| Density of the absorber plate (ρ_p) | 8300 kg.m^{-3} |
| Density of the insulation (ρ_i) | 36 kg.m^{-3} |

| | |
|--|------------------|
| Density of the fluid (ρ_f) | 1000 $kg.m^{-3}$ |
| Emissivity of the carbon black absorber plate (ϵ_p) | 0.92 |
| Absorptivity of the carbon black absorber plate (α) | 0.92 |
| Emissivity of the glass cover (ϵ_c) | 0.88 |

Discretization grids

| | |
|----------------|---------|
| Cover | 11*11 |
| Absorber plate | 11*11 |
| Insulation | 11*11*8 |
| Fluid | 11 |
| Δt | 60 s |

Miscellaneous

| | |
|--|--------|
| Reflectivity of the surrounding (ρ) | 0.2 |
| Collector plate tilt (β) | 24° |
| Latitude of kanpur (ϕ) | 26.28° |

References

- [1] Agarwal M.P.,1996, " Numerical Modelling of Flat Plate Solar Collector : a Multidimensional Approach", M.Tech Thesis, Department of Mechanical Engineering, IIT Kanpur.
- [2] Buchberg H., Catton I. and Edwards D.K., 1976, "Natural Convection in Enclosed Spaces - A review of Applications to Solar Energy Collection", Journal of Heat Transfer, Trans. ASME, Vol.98, pp. 182.
- [3] Brian P.L.T.,1961, "A finite-difference method of high-order accuracy for the solution of three-dimensional transient heat conduction problem." A.I.Ch E.Journal, Vol.7, pp.367-370.
- [4] Chiou J.P.,1982, " The effect of nonuniform fluid flow distribution on the thermal performance of a solar collector", Solar Energy, Vol.29, pp487-502.
- [5] Desai N.I., 1985, " Design development and performance study of a large size solar water heating system" , M.Tech. Thesis, Department of Mechanical Engineering, IIT Kanpur.
- [6] Duffie J.A. and Beckman W.A., "Solar energy Thermal Processes", John Wiley, New York, 1980.
- [7] Goyal Anurag, 1992 , " Experimental investigation of a V-groove solar air heater ", M.Tech. Thesis, Department of Mechanical Engineering, IIT Kanpur.

- [8] Hottel H.C. and Woertz, 1942, "The performance of flat plate solar heat collectors", Trans. ASME Vol.64, pp.91-93.
- [9] Inaba H. and Kanayama K., 1984, "Natural convective heat transfer in an inclined rectangular cavity", JSME, Vol.27, pp.1702-1708.
- [10] Kern J. and Harris I., 1975, "On the optimum Tilt of a Solar Collector", Solar Energy, Vol.17, pp. 97.
- [11] Morse R. N. and Czarnecki, 1958, "Flat-Plate Solar Absorbers : The Effect on incident Radiation of Inclination and orientation", Report E.E.6, Mechanical Engineering Division, C.S.I.R.O., Melbourne.
- [12] Oliva A., Costa M. and Perez Segarra C.D., 1988, "Two and three-dimensional aspects in the thermal behaviour of solar collectors", Adv.Solar Energy Tech., Vol2, pp.1076-1080.
- [13] Saito A., Utake Y., Tsuchio T. and Katayama K., 1984, "Transient response of flat plate solar collectors for periodic solar intensity variation", Solar Energy, Vol.32, pp.17-23.
- [14] Siegel R. and Howell J.R., "Thermal radiation heat transfer", McGraw Hill, New York, 1972.
- [15] Sastry S.S., "Introductory methods of numerical analysis", Tata McGraw Hill, New Delhi, 1994.
- [16] Smith J.G., 1986, "Comparison of transient models for flat plates and trough concentrators", J.Solar Energy Eng., Vol.108, pp.341-344.

- [17] Sukhatme S.P.,1984,"Solar Energy",Tata Mcgraw Hill, New Delhi,1984.
- [18] Suchreke H. and McCormick P.G., 1988, "The diffuse fraction of instantaneous solar radiation ", Solar Energy, Vol.40, pp 423-430.
- [19] Thomas L.H., 1949, " Elliptic problems in linear difference equations over a network", Trans. ASME, Vol.69, pp90-96.
- [20] Threkelde J.L. and Jordon R.C., 1958, "Direct solar radiation available on clear days", ASHRAE Transactions", 64,65.
- [21] Wong H.Y., " Heat transfer for Engineers", Longman, New York, 1977.